

*This is a pre-copy-editing, author-produced PDF of an article accepted for publication in Systematic Biology following peer review. The definitive publisher-authenticated version is available online at:*

<http://dx.doi.org/10.1093/sysbio/syr088>

---

## **Biogeography Revisited with Network Theory: Retracing the History of Hydrothermal Vent Communities**

Yann Moalic<sup>1</sup>, Daniel Desbruyères<sup>1</sup>, Carlos M. Duarte<sup>2, 3</sup>, Alejandro F. Rozenfeld<sup>2</sup>, Charleyne Bachraty<sup>4</sup> and Sophie Arnaud-Haond<sup>1,\*</sup>

<sup>1</sup> Département Etude des écosystèmes profonds (DEEP), IFREMER, Institut Français de Recherche pour l'Exploitation de la Mer, centre de Brest, BP70, 29280 Plouzané, France; E-mail: [Yann.Moalic@ifremer.fr](mailto:Yann.Moalic@ifremer.fr); [Daniel.Desbruyeres@ifremer.fr](mailto:Daniel.Desbruyeres@ifremer.fr)

<sup>2</sup> Department of Global Change Research, IMEDEA, IMEDEA (CSIC-UIB), Instituto Mediterraneo de Estudios Avanzados, 07190 Esporles, Mallorca, Spain; E-mail: [carlosduarte@ifisc.uib.es](mailto:carlosduarte@ifisc.uib.es); [alex@ifisc.uib.es](mailto:alex@ifisc.uib.es)

<sup>3</sup> The UWA Oceans Institute, University of Western Australia, 35 Stirling Highway, Crawley 6009, Western Australia, Australia

<sup>4</sup> Département de sciences biologiques, Université de Montréal, C.P. 6128, succursale Centre Ville, Montreal, Québec, Canada H3C 3J7; E-mail : [charleyne.bachraty@umontreal.ca](mailto:charleyne.bachraty@umontreal.ca)

\*: Corresponding author : Sophie Arnaud-Haond, email address : [Sophie.Arnaud@ifremer.fr](mailto:Sophie.Arnaud@ifremer.fr)

---

### **Abstract:**

Defining biogeographic provinces to understand the history and evolution of communities associated with a given kind of ecosystem is challenging and usually requires a priori assumptions to be made. We applied network theory, a holistic and exploratory method, to the most complete database of faunal distribution available on oceanic hydrothermal vents, environments which support fragmented and unstable ecosystems, to infer the processes driving their worldwide biogeography. Besides the identification of robust provinces, the network topology allowed us to identify preferential pathways that had hitherto been overlooked. These pathways are consistent with the previously proposed hypothesis of a role of plate tectonics in the biogeographical history of hydrothermal vent communities. A possible ancestral position of the Western Pacific is also suggested for the first time. Finally, this work provides an innovative example of the potential of network tools to unravel the biogeographic history of faunal assemblages and to supply comprehensive information for the conservation and management of biodiversity.

**Keywords:** Biogeography, deep sea ecology, hydrothermal vents, network analysis, systems biology

1           Biogeographic provinces are areas of animal and plant distribution that have  
2 similar or shared characteristics throughout. Distinct provinces support different biomes  
3 resulting from divergent ecological and/or evolutionary processes. The identification of  
4 biogeographic provinces and their delimitation are important goals within biogeography,  
5 but such work is seldom straightforward. This is illustrated by the diversity of approaches  
6 that have been proposed for this task (Hausdorf, 2002; Hausdorf and Hennig, 2003;  
7 Nelson and Platnick, 1981), which often involve a somewhat arbitrary delimitation of  
8 boundaries (Hausdorf, 2002) such as the ones based on the geographical distribution of  
9 sites. Approaches are needed that limit the *a priori* hypotheses about the predominant  
10 factors that shape provinces, and therefore deliver more objective delineations of  
11 biogeographic provinces and the pathways of connectivity between them. Network  
12 analysis appears to be a promising tool, as it can help us to understand geographical  
13 landscape connectivity (Dos Santos et al., 2008; McRae and Beier, 2007; Urban and  
14 Keitt, 2001) and genetic relationships between populations or individuals (Rozenfeld et  
15 al., 2007; Rozenfeld et al., 2008). Networks provide representations of complex datasets  
16 where nodes (e.g., communities) are interconnected by links that are scaled to the  
17 connectivity between them, as indicated by metrics of distances or the degree of  
18 interaction between nodes, all of which depend on the system under analysis. The  
19 topology of the ensuing network can then be analysed with a range of tools and models  
20 developed in network theory, allowing inferences on the past or present dynamic  
21 properties of the system. Network analysis provides a holistic approach, free of *a priori*  
22 dataset assumptions, which is better than classical pairwise interaction analyses for  
23 assessing interactions within complex datasets (Proulx et al., 2005). Therefore, network

1 analysis has been shown to be a powerful tool for understanding the behaviour of  
2 biological systems composed of interacting units, with nodes representing units from  
3 genes to communities, and links illustrating their interactions. Analysis of biological  
4 systems as complex networks has allowed, for example, an understanding of species  
5 specialization in mutualistic interactions (Bascompte and Jordano, 2007), species  
6 interactions in a food web (Krause et al., 2003), and the identification of specific  
7 molecules with a crucial role in the stability of specific metabolic pathways (Albert et al.,  
8 2000; Sales-Pardo et al., 2007; Strogatz, 2001). At the intra-specific scale, network  
9 analysis has allowed the elucidation of genetic relationships and structure among  
10 individuals or populations, and provided important insights into dispersal migration  
11 (Fortuna et al., 2009; Rozenfeld et al., 2007), and source-sink dynamics (Rozenfeld et al.,  
12 2008). At the community level, network analysis has allowed the identification of  
13 differentiated communities and biogeographic entities along a continuously-distributed  
14 space, based on patterns of sympatry (Dos Santos et al., 2008).

15         Here, we use network analysis to resolve the biogeography of hydrothermal vent  
16 sites discretely scattered along oceanic ridges, using the faunal composition of 63 such  
17 fields (Desbruyères et al., 2006b). Hydrothermal vents occur across all oceans due to  
18 volcanic activity at active deep-sea ridges, back-arc spreading centers, volcanic arcs and  
19 fore-arcs, and some intraplate seamounts. Widely spaced and often ephemeral, these  
20 ecosystems develop in the darkness of the oceans. They depend almost entirely on  
21 prokaryote chemosynthesis, which allows the proliferation of a specialized fauna  
22 exhibiting limited biodiversity but extraordinarily high biomass (Van Dover, 2000). Since  
23 the initial discovery of vent ecosystems in 1977 (Corliss et al., 1979), research has

1 strongly focused on the origins and processes driving the distribution patterns and  
2 dynamics of the impressive communities they support. The fauna present at hydrothermal  
3 sites appears to be strongly endemic, with only 8 % of species previously found outside  
4 the vent habitat (McArthur and Tunnicliffe, 1998). First discovered on the East Pacific  
5 Rise (EPR) (Hekinian et al., 1983; Spiess et al., 1980), hydrothermal vent fields have now  
6 been found over all of the world's ocean ridges. Other chemosynthetically-based  
7 ecosystems, such as cold seeps and whale carcasses, have also been found to share  
8 common taxa with hydrothermal vents. Increased knowledge of hydrothermal vent  
9 distribution across the ocean floor has prompted interest about the origins, evolutionary  
10 history, and dynamics of these very unusual ecosystems, which rely on the  
11 chemosynthetic production of organic matter.

12         Due to high species endemism, it has been rather difficult to define  
13 comprehensive clusters of biogeographic provinces that could help to reconstruct the  
14 evolutionary history of hydrothermal vent ecosystems. Indeed, the number of distinct  
15 biogeographic provinces recognized ranges between 4 and 7, depending on the number of  
16 vent fields explored and the methods and the underlying hypotheses used to delineate  
17 them (Desbruyères et al., 2006a; Tunnicliffe, 1997; Van Dover et al., 2002). Most  
18 approaches relied on *a priori* hypotheses about faunal composition, geographical  
19 distance, ridge history, topography, and vicariant events, or on an arbitrary defined  
20 cutting distance in UPGMA trees, to cluster hydrothermal sites into provinces. For  
21 example, in different studies, the East Pacific Rise has been considered to contain one  
22 (Van Dover et al., 2002), two (Bachraty et al., 2009) or three (Tunnicliffe, 1997)  
23 biogeographic provinces, depending on the underlying hypothesis and information. The

1 similarities in hydrothermal vent assemblages are particularly important because, in  
2 addition to helping delineate biogeographical provinces, they can also help elucidate the  
3 links between different biogeographical provinces, which may contribute to  
4 understanding their history and colonization pathways, and the dispersal patterns of the  
5 fauna they contain. The extreme level of endemism across vent sites can be attributed to  
6 (i) the partial colonization of limited ridge segments by some species, and (ii) the  
7 divergence of species over geological time. The occurrence of a large number of common  
8 genera, represented by different species across vent sites, supports the idea of vicariance  
9 as one of the main drivers of the spatial heterogeneity observed in community  
10 composition (Tunnicliffe et al., 1998), resulting from species divergence on both sides of  
11 geographical barriers such as major ridge discontinuities or transforming faults (Plouviez  
12 et al., 2009). High endemism, combined with the extremely fragmented distribution of  
13 vents along Mid-oceanic Ridges, means that the Network Analysis Method (NAM)  
14 proposed by Dos Santos et al. (2008), is not possible based on species; nor was it  
15 necessary, as the fragmented distribution of sites offers a natural delineation of  
16 geographic units (i.e., hydrothermal fields).

17 An alternative approach to examine the relationships between the hydrothermal  
18 vent fauna can be taken, using network analysis to represent each of the 63 hydrothermal  
19 vent fields, investigated to date, as nodes can be connected among them with a distance  
20 reflecting the common genera among sites (links). These networks of hydrothermal vent  
21 communities can then be formally analyzed to explore their structures; identifying groups  
22 of closely-related locations that are helpful in delineating biogeographic provinces and  
23 the hydrothermal vent regions connecting these provinces. Moreover, such networks can

1 be constructed without entering any information concerning the geological or geographic  
2 properties of the sites, thereby allowing subsequent examination of the consistency  
3 between the network structure and the independent geological or geographic properties as  
4 a validation exercise. In particular, we aimed at testing i) the various delineation of  
5 biogeographic provinces hitherto proposed by different authors, and ii) the hypothesis of  
6 an ancient history of colonization and evolution of hydrothermal communities by  
7 comparing the pattern of clustering and connectivity revealed by network analysis with  
8 the spreading of oceanic ridges across geological time (Desbruyères et al., 2006a;  
9 Tunnicliffe, 1997; Van Dover et al., 2002).

10

## 11 MATERIALS AND METHODS

### 12 *Dataset used in this study*

13 Hydrothermal vent fields (n=63) were selected across the world's oceans  
14 according to available information on their faunal composition. A taxonomic database  
15 from a recent compilation (Desbruyères et al., 2006b), was assembled from information  
16 from the literature, databases on the World Wide Web (ChEss:  
17 <http://www.noc.soton.ac.uk/chess/database/>, NOAA: <http://www.pmel.noaa.gov/>, NeMO:  
18 <http://www.pmel.noaa.gov/vents/nemo/>), and researchers we contacted directly. At each  
19 of the 63 hydrothermal vent fields, the presence or absence of taxa was noted among the  
20 total 591 species and 331 genera described. All the taxa recorded in the biogeographic  
21 provinces found by network analysis are described in Supplementary Table 1 (available  
22 from <http://www.sysbio.oxfordjournals.org>).

### 23 *Networks*

1           We began analysis with a fully connected network of 63 hydrothermal vent fields  
2 considered as nodes. Each link joining a pair of fields was assigned the corresponding  
3 Jaccard's index distance. This assemblage distance is given by:

4           Jaccard's index distance =  $1 - \left( \frac{a}{a + b + c} \right)$ ,

5           where  $a$  is the number of taxa (i.e., genera or species) common to two fields (for example  
6 field 1 and field 2),  $b$  is the total number of taxa present in field 1 but absent from field 2,  
7 and  $c$  is the total number of taxa present in field 2 but absent from field 1.

8           This coefficient ranges from 0 (both fields are identical) to 1 (the fields share no  
9 items) and gives similar weight to the presence or absence of a taxon. This property  
10 makes the Jaccard's index distance more appropriate for the present case because the  
11 available description of these remote communities is far from exhaustive, and some  
12 absences may also be due to the lack of observation of a given taxon, rather than to true  
13 absences from the community. Nevertheless, when tests with Sorensen index, which  
14 gives double weighting to double presence, were realized on the same dataset, results  
15 yielded a similar network topology, with identical clusters. Consequently, we kept the  
16 simplest index and focused on analyses at different taxonomic levels. Therefore, we  
17 analyzed and compared networks of Jaccard's index at both the species and genus levels.  
18 Like previous authors (Tunncliffe et al., 1996), we consider that genus-level analysis  
19 provides a more appropriate picture of the patterns of dispersal and/or vicariance between  
20 hydrothermal fields, based on the high levels of endemism observed at the species level.  
21 Jaccard distance interpretation in this context is that hydrothermal vent areas once  
22 connected by strongest dispersal paths would have exchanged more species, resulting in a

1 lower Jaccard distance at both species and genus levels among contemporary  
2 communities.

3 The similarity matrix provides a fully-connected network that does not allow  
4 recognition of biogeographic provinces. Various approaches have been developed to  
5 extract biogeographic provinces from networks, including those based on community  
6 detection (Allesina and Pascual, 2009; Krause et al., 2003; Newman, 2004) and  
7 percolation theory (Rozenfeld et al., 2008). A percolation approach was used to break  
8 down the fully-connected network into discrete clusters of biogeographic provinces  
9 because these are better able to handle continuous link weights (Jaccard's index distance).  
10 Moreover, Rozenfeld *et al.* (2008) successfully applied the percolation distance approach  
11 to resolve gene flow within species, based on a fully-connected network of populations.  
12 We transposed this method to the community level to resolve the biogeographic  
13 provinces emerging from historical disruption of gene flow through ancient vicariant  
14 events.

15 The percolation method is based on the analysis of a network built only with links  
16 illustrating the minimum Jaccard distance necessary to maintain the connexion across  
17 most components of the system. At this distance precisely, the network still depicts a  
18 single, giant cluster composed of sub-clusters linked through primary connections. Below  
19 this distance, the network collapses into disconnected sub-clusters, and the pattern of  
20 global connectivity is lost. This critical threshold distance is also named percolation  
21 distance ( $D_p$ ); (Stauffer and Aharony, 1994). For a finite system, this point is derived by  
22 calculating the average cluster size of all clusters excluding the largest,

23 
$$\langle S \rangle^* = \frac{1}{N} \sum_{s \in \{S \max\}} s^2 n_s,$$

1 as a function of the last threshold distance value beyond which links were removed.  $N$  is  
2 the total number of nodes not included in the largest cluster and  $n_s$  is the number of  
3 clusters containing  $s$  nodes.  $S_{max}$  is the size of the largest cluster. The  $D_p$  is then  
4 identified heuristically in the transitional region characterized by a strong decrease in  
5  $\langle S \rangle^*$ . Inside this transitional stage, the single, giant cluster network is found at  $D_p=0.84$ .  
6 The network topology and its characteristics were analyzed at this percolation distance,  
7 meaning that the links retained in the network analyzed are the ones corresponding to  
8 ecological distances lower or equal to  $D_p$ , while all links beyond that value were  
9 discarded. Additionally, the network was also explored at different distance thresholds  
10 around this percolation point, in order to assess the consistency of its topology and the  
11 inferred properties and interpretation. The network characteristics (see Glossary) were  
12 quite robust to variability with the applied threshold distance  $D_p$ : major clusters, nodes  
13 and paths remained unchanged indicating in the robustness of these key properties to  
14 uncertainty in the percolation threshold and, therefore, supporting the reliability of the  
15 network for displaying the biogeographic structure of the communities.

16 In order to assess the respective influence of the three main phyla that encompass  
17 more than 80 % of the genera (Annelida, Mollusca and Arthropoda, which represent 20.5  
18 %, 25 % and 37 %, respectively) on the global network topology, three sub-networks  
19 were then built based on genera within these three major phyla.

20

21 *Estimation of the global and local properties of the network*— The *connectivity*  
22 *degree*,  $k_i$  of a given node  $i$ , is the number of other nodes linked to it (i.e., the number of  
23 neighbor nodes). We named  $E_i$  as the number of links existing among the neighbors of

1 node  $i$ . This quantity takes values between 0 and  $E_i^{(\max)} = k_i(k_i-1)/2$ , which is the case in a  
2 fully connected neighborhood. This value is used to calculate the *clustering coefficient*  $C_i$   
3 of node  $i$ , defined as:

$$4 \quad C_i = \frac{E_i}{E_i^{(\max)}} = \frac{2E_i}{k_i(k_i-1)},$$

5  $C_i$  quantifies how close the node  $i$  and its neighbors are to being a clique (See  
6 Supplementary Fig. 1a for an illustrative diagram). The *clustering coefficient* (Watts and  
7 Strogatz, 1998) of the whole network  $\langle CC \rangle$  is defined as the average of all the individual  
8 clustering coefficients in the system.  $C_i$  values vary between 0 and 1. The *clustering*  
9 *coefficient* helps us to understand how nodes are organized into clusters within the system  
10 as a whole. In order to test the significance of  $\langle CC \rangle$ , its value was compared to the  
11 average value  $\langle CC_o \rangle$  of 10 000 random simulations of our dataset. To perform this test,  
12 we randomly rewired our network with the same number of links present at a given  
13 threshold (here percolation), thereby yielding random networks with the same overall  
14 structure of taxa presence and absence.

15 The *betweenness centrality* (Freeman, 1977) of node  $i$ ,  $bc(i)$ , counts the fraction of  
16 shortest paths between pairs of nodes that pass through node  $i$ . Let  $\sigma_{st}$  denote the number  
17 of shortest paths connecting nodes  $s$  and  $t$ , and  $\sigma_{st}(i)$  the number of those passing through  
18 the node  $i$ ; then,

$$19 \quad bc(i) = \sum_{s \neq t \neq i} \frac{\sigma_{st}(i)}{\sigma_{st}}.$$

20 The *betweenness centrality* determines the relative importance of a node within the  
21 network as an intermediary in the flow of information and its vulnerability to  
22 fragmentation (See Supplementary Fig. 1b for an illustrative schema).

1            Networks were visualized and analysed using Pajek software (Batagelj and Mrvar,  
2 2002). Random simulations were compiled by C++ scripts.

3

4            *Comparative analysis*— A set of four methods based on community detection  
5 were additionally tested on this dataset to infer their potential for biogeographic analysis  
6 on our dataset (Blondel et al., 2008; Dongen, 2008; Girvan and Newman, 2002; 2008).  
7 See Supplementary Table 2 for details on these methods.

## 8 RESULTS

### 9 *Delineation of Biogeographic Provinces*

10            In order to reveal the clustering and interconnectivity of hydrothermal vents, we  
11 built networks with data from the 63 fields (nodes) referenced in the database (See  
12 Supplementary Table 3), connected by links (edges) on the basis of their faunal distance  
13 in terms of genera, as assessed with Jaccard's index in an adjacency matrix (Legendre  
14 and Legendre, 1998). Genera were chosen, rather than species, because of the extremely  
15 high level of endemism at the species level (95.3 %, compared with 76.2 % for genera;  
16 see Supplementary Fig. 2), indicating that biogeographic history is ancient and likely to  
17 be better reflected by the distribution of genera (Tunncliffe and Fowler, 1996).

18            The Jaccard's distances were, as expected, lower for neighbouring vent sites but  
19 the resulting network had a percolation value at a Jaccard distance of  $D_p=0.84$ , below  
20 which distinct groups of vent sites emerged suggesting distinct biogeographic regions  
21 (Fig. 1). In particular, the network topology clearly shows the existence of 5 strong  
22 clusters of hydrothermal vents (Fig. 1 and Fig. 2, see Table 1 for the network properties),  
23 even though the data used contained no geographic information and the process did not

1 involve any subjective dissection like those needed for a ‘classic’ dichotomic UPGMA  
2 tree (See Supplementary Fig. 3). The ensuing clusters of hydrothermal vents correspond  
3 to five well-defined regional provinces, coherent both at the genus (Fig. 2) and species  
4 (Supplementary Fig. 4 and 5) levels, in agreement with Tunnicliffe *et al.* (1998). At the  
5 species level, the network topology loses its integrity at a Dp value higher than the one  
6 of the genus level (0.95 vs 0.84). This is due to the high species endemism; the much  
7 lower number of shared species than genera among fields results in a higher threshold  
8 below which the connectivity across the entire network breaks down (Supplementary Fig.  
9 5).

10         Analyses performed at the genus level showed that this hierarchical structure is  
11 supported by a significantly higher average clustering coefficient,  $\langle CC \rangle = 0.52$ , than  
12 expected by chance (i.e., by randomly rewiring the links ( $\langle CC_o \rangle = 0.17$  with  $\sigma_o = 0.01$ , after  
13 10 000 random simulations), thus illustrating the modularity of the network composed of  
14 clusters of hydrothermal fields, with greater internal interconnection than would be  
15 expected by chance. Moreover, the recognition of the West Pacific (WP), Northeast  
16 Pacific (NP), East Pacific Rise (EPR), and Mid-Atlantic Ridge (MAR) as provinces is  
17 confirmed by their individual  $\langle CC \rangle$  values, which are higher than the average (Table 1).  
18 This highlights the strong endemism of hydrothermal vent fauna among the provinces  
19 defined by the network clusters (Fig. 2).

#### 20 *Connectivity among Provinces*

21         In addition to an objective identification of biogeographic provinces and sub-  
22 provinces, network analysis offers another fundamental advantage: the study of  
23 biogeographic patterns in hydrothermal fields as the patterns of connectivity among fields

1 and provinces can suggest past and present dynamics of information flow reflecting  
2 species divergence. Putative pathways can be assessed from the connections among  
3 biogeographic provinces in the network topology, identifying regions that possibly play  
4 or have played a role in the foundation and/or connectivity of the system. The first  
5 observation that emerges when these 'inter-cluster' links are considered is the central  
6 position of the WP province. WP is intermediate among all other provinces, which  
7 themselves share no links (Fig. 2). An accurate diagnostic for this analysis is the  
8 *betweenness centrality* (see Materials and Methods), which estimates the relative  
9 importance of a node in relaying the flow of information through the system,  
10 corresponding here to past gene flow, which will result in common genera across fields  
11 represented in the network (Fig 2 and Supplementary Table 4). Here, the two strongest  
12 *betweenness centrality* values indeed correspond to fields in the WP region: the Mariana  
13 Trough and the Pacmanus system, which are present in 28 % and 26 %, respectively, of  
14 all shortest paths among fields. As noted above, the MAR province has no direct link  
15 with EPR, so that the Eastern Pacific and Atlantic Oceans are only connected in the  
16 network through the West Pacific and Indian Oceans.

17 The taxon-specific networks represented in Supplementary Fig. 6 show slightly  
18 lower percolation threshold than the global network ( $D_p = 0.84$ ) revealing a higher  
19 overall proximity of communities of Annelida ( $D_p = 0.68$ ), Arthropoda ( $D_p = 0.77$ ), and  
20 Mollusca ( $D_p = 0.75$ ) but generally support the number and identity of the biogeographic  
21 provinces revealed by the global network. These patterns are clearly similar for Annelida  
22 and Arthropoda (Supplementary Fig. 6a and 6b) with the same five provinces  
23 distinguished. For Mollusca (Supplementary Fig. 6c), WP, MAR, and EPR provinces still

1 appear as a single cluster with NP divided into two clusters connected either to WP or to  
2 EPR, and IO disconnected.

3

#### 4 *Comparative Analysis*

5       Among the methods tested based on community detection, only the method from  
6 Rosvall and Bergstrom (2008) showed resolution and cluster discrimination, while no  
7 coherent clusters emerged with the other methods (see Supplementary Table 1). The  
8 analysis with the Rosvall and Bergstrom (2008) method shows a lower resolution than the  
9 percolation approach, while still supporting the discrimination of NP and EPR, and their  
10 sequential branching with and through the cluster including WP (merged with MAR and  
11 IO).

## 12 DISCUSSION

13       The overall picture of hierarchical structure and connectivity among vent sites  
14 depicted by this network analysis allows the definition of five biogeographic provinces at  
15 the percolation threshold distance of the network, which is defined on the basis of the  
16 global analysis of taxonomic similarity among sites. Compared to previous studies based  
17 on other approaches that rely on a more ‘arbitrary’ identification of clusters, some  
18 previously-recognized distinct provinces appear to be compounded into a single one here,  
19 while others are well differentiated. In fact, the splitting of EPR or MAR proposed in  
20 previous studies (Tunnicliffe, 1997; Van Dover et al., 2002) is not supported here for  
21 MAR (Fig. 1) which corresponds, at best, to slightly differentiated sub-provinces for  
22 EPR, disconnecting at a threshold far lower than that at which the other provinces are  
23 identified (just before the threshold of 0.60; Fig. 1a). The integrity of the IO province

1 remains questionable due to its extremely weak representation in the data gathered so far,  
2 due to a lack of scientific cruises in this area. The two fields explored in IO do however  
3 remain strongly linked together, which, coupled with the robust intermediate position of  
4 IO between MAR and WP (Fig. 2), strongly supports the existence of at least one discrete  
5 province in this region.

6         The central position of WP in all connection paths between provinces was  
7 supported both by the global analysis at the genus and species (Supplementary Fig. 4)  
8 levels, by the analysis specific to each of the three main phyla (Annelida, Mollusca, and  
9 Arthropoda). The network topology derived here calls into question the hypothesis of a  
10 major ancestral pathway between the EPR and MAR provinces through the Isthmus of  
11 Panama as well as the hypothesized connectivity between the Eastern Pacific and the  
12 Southern Atlantic through the Circumpolar Current (Van Dover et al., 2002).

13

#### 14 *Network Consistency with Tectonic History*

15         The star-like topology of the network (Fig. 2), characterised by a central position  
16 of WP (formally reflected in its high betweenness-centrality score in the network), results  
17 in the lack of direct connection between EPR and NP at the percolation threshold, which  
18 suggests a more recent common history of WP with each of these provinces  
19 independently.

20         The topology derived here shows some similarity to the early history of the plate  
21 tectonic and spreading ridge system in the Pacific during the Mesozoic and its evolution  
22 over more than 100 million years (see Fig. 3). Although this consistency does not  
23 necessarily involve a causal relationship, it lends weight to the hypothesis that the current

1 biogeographic structure of hydrothermal vent fauna may have been influenced by the  
2 tectonic dynamics of plates over millions of years (Hessler and Lonsdale, 1991;  
3 Tunnicliffe et al., 1996). Indeed, the double network connection of EPR and NP  
4 exclusively through WP, which also appeared when using the community detection  
5 method of Rosvall and Bergstrom (2008, Supplementary Table 2), is consistent with the  
6 history of the Pacific ridge since the early Cretaceous (~150 Ma), and the split of the  
7 protoridges triple junction during the end of the Cretaceous (~70 Ma) and Paleocene (~60  
8 Ma; Fig. 3) (Smith, 2003). The branching of EPR on WP observed in the network (Fig.  
9 2) is also consistent with the early Cretaceous position of the three ridges (Izanagi-  
10 Farallon, Pacific-Izanagi, and Pacific-Farallon), connecting the West and the South  
11 Eastern Pacific (Fig. 3a), until their disconnection by a fracture zone in the Late  
12 Cretaceous (Fig. 3c). Finally, the network connection of NP to WP can also be considered  
13 in parallel with the early history of the Juan de Fuca Ridge, which appeared during the  
14 Paleocene and was connected to WP and the future EPR at the time when the ridge triple  
15 junction splits the Pacific, Kula, and Farallon plates.

16         It is obviously impossible to test this hypothesis experimentally, so the direct  
17 influence of the tectonic plate history on the present nature and distribution of  
18 hydrothermal communities, while consistent with the topology of the network built here,  
19 remains speculative. Nevertheless, it deserves to be examined in further studies, such as  
20 through the construction of complete phylogenies of some of the most widespread genera,  
21 with appropriate markers allowing the use of relaxed molecular clocks.

22

1 *Hubs, Connectivity and Centrality*

2           The central position of WP in the network as an obligatory relay between EPR  
3 and the other provinces (Fig. 2), contrasts with the hypothesis of a center of dispersion in  
4 EPR (Bachraty et al., 2009; Van Dover, 2000; Van Dover and Hessler, 1990). This may  
5 be due to the use of the Jaccard's distance as, in contrast to other distance metrics such as  
6 the dispersal direction coefficient (Bachraty et al., 2009), for example, which comes with  
7 the underlying hypothesis that richest provinces disperse more, Jaccard distance does not  
8 impose an underlying hypothesis linking richness to present or past connectivity. The  
9 EPR appears as the richest province in the database, both in terms of species and genera.  
10 Yet, rather than a high divergence rate and dispersal towards adjacent provinces, this  
11 richness may reflect the combination of different sampling strategies among provinces  
12 and the homogeneous topology of EPR.

13           The homogeneity and high connectivity in EPR is illustrated by its robustness in  
14 the network. As the threshold distance declines, the cohesion of each biogeographic  
15 province collapses in the sequence: WP, MAR, NP, EPR (Fig. 1), with EPR still strongly  
16 clustered long after the other provinces collapse (Fig. 1a). This homogeneity is illustrated  
17 by its much larger average *connectivity degree* (See Methods;  $k = 7.81$  for  $n = 17$  vents  
18 observed; Table 1) that reveals the relatively low level of endemism within this province  
19 (Supplementary Fig. 2). This may be the result of the specific regional properties of the  
20 EPR fields (Fig. 4) that exhibit a high accretion rate (rate of creation of new oceanic  
21 lithosphere) inducing a higher number of vents (Baker et al., 1995), a factor which,  
22 associated with a homogeneous depth is likely to facilitate the faunal dispersion. The  
23 relative homogeneity of EPR is also reflected by a rather low genetic structure and

1 significant gene flow estimates for several taxa studied across EPR, the area where the  
2 most population genetic studies have been performed to date (Chevaldonné et al., 1997;  
3 Hurtado et al., 2004; Jollivet et al., 1999; Matabos et al., 2008; Vrijenhoek, 1997); a  
4 result in line with the relative ubiquity of taxa in this province (Supplementary Fig. 2). In  
5 contrast, the WP province shows a much higher level of endemism, as shown by a much  
6 lower average *connectivity degree* ( $k=4.53$ ), despite the greater number of referenced  
7 vent fields ( $n=26$ ). Moreover, the EPR has been the specific target of numerous cruises,  
8 allowing the examination of extinction and recolonization processes (Lutz et al., 1994), as  
9 well as the discovery and description of taxa of distinct succession stages. As a result,  
10 despite its apparently high richness in comparison with some previous studies (Bachraty  
11 et al., 2009; Van Dover, 1995; Van Dover, 2000), EPR does not emerge as an especially  
12 central cluster of nodes (province) in this network, which instead supports a central  
13 position for WP.

14         This central position of WP, both at the scale of the Pacific Ocean and worldwide,  
15 combined with its extremely high endemism, suggests a more ancient history and a  
16 central role in the biogeography of hydrothermal vents. WP is the region of the world  
17 where the basins exhibit the highest bathymetric variability of vents (Fig. 4), compared  
18 with mid-ocean ridges (Matabos et al., 2008), and where closely located vents and seeps  
19 coexist most frequently (Sibuet and Olu, 2002). There is recent evidence suggesting that  
20 the colonization of deep chemosynthetic ecosystems may have followed a stepping stone  
21 model from the coastal area, through sunken wooden debris and large animal carcasses,  
22 to the cold seeps and finally the hydrothermal vents (Van Dover et al., 2002). Such  
23 findings agree with inferences drawn by Little and Vrijenhoek (2003) on fossil and

1 molecular evidence. Observations supporting this stepping stone hypothesis were first  
2 reported on the mytilidae (Distel et al., 2000; Samadi et al., 2007). Altogether, (i) the  
3 heterogeneity of WP field depth and their close proximity to seeps (active margins),  
4 fallen wood (tropical islands), and the coastal zone, (ii) their pattern of within-region  
5 endemism and ancient divergence among taxa on this old, slow-spreading ridge, and (iii)  
6 their central position in the topology of the network reported here, support the hypothesis  
7 of a colonization or recolonization of hydrothermal vents through WP, followed by a  
8 subsequent worldwide dispersion that was possibly influenced by plate tectonics and the  
9 associated evolution of spreading ridge systems since the early Mesozoic (Desbruyères et  
10 al., 2006a). This hypothesis could also be worthy of future testing using phylogenetic  
11 reconstructions.

12

### 13 *Origin and Ageing of Communities*

14         The reconstruction of the ageing and history of vent taxa to date has been based  
15 either on fossils or molecular clocks, which produced contradictory estimates (Little and  
16 Vrijenhoek, 2003). The oldest fossils from the Paleozoic (~450 Ma) and the high  
17 endemism of hydrothermal communities led to an ‘antiquity hypothesis’ (Newman,  
18 1985). Molecular data, in contrast, supported a much more recent history, even when  
19 considering a slow molecular clock calibrated on the Farallon-Pacific Ridge disruption  
20 under the North-American Plate (Chevaldonné et al., 2002). Reconsidering the evidence  
21 from both molecular and fossil data, Little and Vrijenhoek (2003) suggested that present  
22 hydrothermal fauna were of intermediate age and may have originated in the Mesozoic (-  
23 150 Ma). The network topology described here lends support to their suggestions,

1 showing consistency between the evolution of oceanic ridges since the early Cretaceous  
2 and the topology of the network that illustrates the nature and connections among  
3 biogeographic provinces. It is also in agreement with a role of shallow hydrothermal  
4 vents and close cold seeps in the (re)colonization of hydrothermal vents. In line with the  
5 geographic location of most fossil records (Little, 2002), the network suggests a high  
6 centrality of the WP region where (re)colonization events may have mainly taken place.  
7 The hypothesized central position of WP and its possible role in the original history of  
8 present day hydrothermal vent fauna derived from network analysis also require further  
9 investigation, which could be done through comprehensive phylogenies of different  
10 genera, to test for whether fauna from WP have the basal position that would be expected  
11 from such an ancestral role.

12

13         The application of network analysis to examine hydrothermal vent biogeography  
14 reported here provides evidence of the potential of this approach to address complex  
15 biogeography problems. First, network analysis allows the discrimination of clusters of  
16 communities, or biogeographic provinces and is genuinely obtained without introducing  
17 additional information, such as *a priori* assumptions on their clustering based on their  
18 geographic location. Second, this holistic approach allows illustrating the connectivity  
19 between provinces with a rather flexible geometry, free of the constraint of the  
20 dichotomous relationship imposed by branching rules in classical trees. Third, network  
21 analysis provides tools developed to derive diagnostics on the dynamics properties of the  
22 network, such as *betweenness centrality*, which allows particular regions or provinces to  
23 be pointed out that may have had a central role in the evolution and dispersion of fauna

1 and, therefore, be of major relevance for biogeographical analyses. The application of  
2 network analysis, already used across a wide range of fields from social science to  
3 ecology, and more recently in population genetics (Fortuna et al., 2009; Rozenfeld et al.,  
4 2008), therefore opens a promising avenue for the investigation of biogeographic  
5 questions. This work takes a first step that we hope may encourage the use of network  
6 analysis, not only with the method presented here but also others, such as community  
7 detection approaches (Fortunato, 2010), among the rapidly broadening and improving  
8 range of network analysis methods.

9

10

## 11 ACKNOWLEDGMENTS

12 We particularly thank Verena Tunnicliffe for helpful suggestions on a preliminary  
13 version of this work, and Helen McCombie for English editing.

14 This work was supported by the EU-funded HERMIONE ('Hotspot ecosystem research  
15 and man's impact on European seas') project, part of the Environment Theme of the  
16 Seventh Framework Programme (FP7) and the French ANR Deep Oases (ANR06  
17 BDV005)

18

## REFERENCES

- Albert, R., H. Jeong, and A. L. Barabasi. 2000. Error and attack tolerance of complex networks. *Nature* 406:378-82.
- Allesina, S., and M. Pascual. 2009. Food web models: a plea for groups. *Ecol Lett* 12:652-62.
- Bachraty, C., P. Legendre, and D. Desbruyères. 2009. Biogeographic relationships among deep-sea hydrothermal vent faunas at global scale. *Deep Sea Research Part I: Oceanographic Research Papers* 56:1371-1378.
- Baker, E. T., C. R. German, and H. Elderfield. 1995. Hydrothermal plumes over spreading-center axes: global distributions and geological inferences. Pages 47-71 *in* *Seafloor Hydrothermal Systems* (R. A. Z. S.E. Humphris, L.S. Mullineaux and R.E. Thomson, ed.) American Geophysical Union.
- Bascompte, J., and P. Jordano. 2007. Plant-Animal Mutualistic Networks: The Architecture of Biodiversity. *Annual Review of Ecology, Evolution, and Systematics* 38:567-593.
- Batagelj, V., and A. Mrvar. 2002. Pajek - Analysis and visualization of large networks. *Graph Drawing* 2265:477-478.
- Blondel, V. D., J. L. Guillaume, R. Lambiotte, and E. Lefebvre. 2008. Fast unfolding of communities in large networks. *Journal of Statistical Mechanics-Theory and Experiment*:-
- Chevaldonné, P., D. Jollivet, D. Desbruyères, R. A. Lutz, and R. C. Vrijenhoek. 2002. Sister-species of eastern Pacific hydrothermal vent worms (Ampharetidae, Alvinellidae, Vestimentifera) provide new mitochondrial COI clock calibration. *Cahiers de Biologie Marine* 43:367-370.

- Chevaldonné, P., D. Jollivet, A. Vangriesheim, and D. Desbruyères. 1997. Hydrothermal-vent alvinellid polychaete dispersal in the eastern Pacific. 1. Influence of vent site distribution, bottom currents, and biological patterns. *Limnology and Oceanography* 42:67-80.
- Corliss, J. B., J. Dymond, L. I. Gordon, J. M. Edmond, R. P. von Herzen, R. D. Ballard, K. Green, D. Williams, A. Bainbridge, K. Crane, and T. H. van Andel. 1979. Submarine thermal springs on the Galápagos Rift. *Science* 203:1073-1083.
- Desbruyères, D., J. Hashimoto, and M. C. Fabri. 2006a. Composition and biogeography of hydrothermal vent communities in Western Pacific back-arc basins. *Geophysical Monograph* 166:215-234.
- Desbruyères, D., M. Segonzac, and M. Bright. 2006b. Handbook of deep-sea hydrothermal vent fauna. Landesmuseen, Linz.
- Distel, D. L., A. R. Baco, E. Chuang, W. Morrill, C. Cavanaugh, and C. R. Smith. 2000. Do mussels take wooden steps to deep-sea vents? *Nature* 403:725-726.
- Dongen, S. V. 2008. Graph Clustering Via a Discrete Uncoupling Process. *SIAM Journal on Matrix Analysis and Applications* 30:121-141.
- Dos Santos, D. A., H. R. Fernandez, M. G. Cuezco, and E. Dominguez. 2008. Sympatry inference and network analysis in biogeography. *Syst Biol* 57:432-48.
- Fortuna, M. A., R. G. Albaladejo, L. Fernandez, A. Aparicio, and J. Bascompte. 2009. Networks of spatial genetic variation across species. *Proc Natl Acad Sci U S A* 106:19044-9.
- Fortunato, S. 2010. Community detection in graphs. *Physics Reports-Review Section of Physics Letters* 486:75-174.

- Freeman, L. C. 1977. Set of Measures of Centrality Based on Betweenness. *Sociometry* 40:35-41.
- Girvan, M., and M. E. Newman. 2002. Community structure in social and biological networks. *Proc Natl Acad Sci U S A* 99:7821-6.
- Hausdorf, B. 2002. Units in biogeography. *Syst Biol* 51:648-652.
- Hausdorf, B., and C. Hennig. 2003. Biotic element analysis in biogeography. *Syst Biol* 52:717-723.
- Hekinian, R., J. Francheteau, V. Renard, R. D. Ballard, P. Choukroune, J. L. Cheminee, F. Albarede, J. F. Minster, J. L. Charlou, J. C. Marty, and J. Boulegue. 1983. Intense hydrothermal activity at the axis of the East Pacific Rise near 13°N: Submersible witnesses the growth of sulfide chimney. *Marine Geophysical Researches* 6:1-14.
- Hessler, R. R., and P. F. Lonsdale. 1991. Biogeography of Mariana Trough Hydrothermal Vent Communities. *Deep-Sea Research Part a-Oceanographic Research Papers* 38:185-199.
- Hurtado, L. A., R. A. Lutz, and R. C. Vrijenhoek. 2004. Distinct patterns of genetic differentiation among annelids of eastern Pacific hydrothermal vents. *Mol Ecol* 13:2603-15.
- Jollivet, D., P. Chevaldonné, and B. Planque. 1999. Hydrothermal-vent alvinellid polychaete dispersal in the eastern Pacific. 2. A metapopulation model based on habitat shifts. *Evolution* 53:1128-1142.
- Krause, A. E., K. A. Frank, D. M. Mason, R. E. Ulanowicz, and W. W. Taylor. 2003. Compartments revealed in food-web structure. *Nature* 426:282-5.

- Legendre, P., and L. Legendre. 1998. Numerical Ecology. Elsevier Scientific Publishing Company.
- Little, C. T. S. 2002. The fossil record of hydrothermal vent communities. *Cahiers de Biologie Marine* 43:313-316.
- Little, C. T. S., and R. C. Vrijenhoek. 2003. Are hydrothermal vent animals living fossils? *Trends in Ecology & Evolution* 18:582-588.
- Lutz, R. A., T. M. Shank, D. Fornari, R. M. Haymon, M. D. Lilley, K. L. Von Damm, and D. Desbruyères. 1994. Rapid growth at deep-sea vents. *Nature* 371:663-664.
- Matabos, M., E. Thiébaud, D. Le Guen, F. Sadosky, D. Jollivet, and F. Bonhomme. 2008. Geographic clines and stepping-stone patterns detected along the East Pacific Rise in the vetigastropod *Lepetodrilus elevatus* reflect species crypticism. *Marine Biology* 153:545-563.
- McArthur, A. G., and V. Tunnicliffe. 1998. Relics and antiquity revisited in the modern vent fauna. Pages 271-291 *in* Modern Ocean Floor Processes and the Geological Record (K. Mills R.A. & Harrison, ed.) Geological Society, London.
- McRae, B. H., and P. Beier. 2007. Circuit theory predicts gene flow in plant and animal populations. *Proc Natl Acad Sci U S A* 104:19885-90.
- Nelson, G., and N. I. Platnick. 1981. Systematics and Biogeography: Cladistics and Vicariance, New York.
- Newman, M. E. 2004. Analysis of weighted networks. *Phys Rev E Stat Nonlin Soft Matter Phys* 70:056131.
- Newman, W. A. 1985. The abyssal hydrothermal vent invertebrate fauna : a glimpse of antiquity? *Bulletin of the Biological Society of Washington* 6:231-242.

- Plouviez, S., T. M. Shank, B. Faure, C. Daguin-Thiebaut, F. Viard, F. H. Lallier, and D. Jollivet. 2009. Comparative phylogeography among hydrothermal vent species along the East Pacific Rise reveals vicariant processes and population expansion in the South. *Mol Ecol* 18:3903-3917.
- Proulx, S. R., D. E. L. Promislow, and P. C. Phillips. 2005. Network thinking in ecology and evolution. *Trends in Ecology & Evolution* 20:345-353.
- Rosvall, M., and C. T. Bergstrom. 2008. Maps of random walks on complex networks reveal community structure. *Proc Natl Acad Sci U S A* 105:1118-23.
- Rozenfeld, A. F., S. Arnaud-Haond, E. Hernandez-Garcia, V. M. Eguiluz, M. A. Matias, E. Serrao, and C. M. Duarte. 2007. Spectrum of genetic diversity and networks of clonal organisms. *J R Soc Interface* 4:1093-1102.
- Rozenfeld, A. F., S. Arnaud-Haond, E. Hernandez-Garcia, V. M. Eguiluz, E. A. Serrao, and C. M. Duarte. 2008. Network analysis identifies weak and strong links in a metapopulation system. *Proc Natl Acad Sci U S A* 105:18824-18829.
- Sales-Pardo, M., R. Guimera, A. A. Moreira, and L. A. Amaral. 2007. Extracting the hierarchical organization of complex systems. *Proc Natl Acad Sci U S A* 104:15224-9.
- Samadi, S., E. Quemere, J. Lorion, A. Tillier, R. von Cosel, P. Lopez, C. Cruaud, A. Couloux, and M. C. Boisselier-Dubayle. 2007. Molecular phylogeny in mytilids supports the wooden steps to deep-sea vents hypothesis. *Comptes Rendus Biologies* 330:446-456.
- Sibuet, M., and K. Olu. 2002. Cold Seep Communities on Continental Margins: Structure and Quantitative Distribution Relative to Geological and Fluid Venting

- Patterns. Pages 235-251 *in* Ocean Margin Systems (Springer-Verlag, ed.), Berlin Heidelberg.
- Smith, A. D. 2003. A reappraisal of stress field and convective roll models for the origin and distribution of cretaceous to recent intraplate volcanism in the Pacific basin. *International Geology Review* 45:287-302.
- Spiess, F. N., K. C. Macdonald, T. Atwater, R. Ballard, A. Carranza, D. Cordoba, C. Cox, V. M. Diaz Garcia, J. Francheteau, J. Guerrero, J. Hawkins, R. Haymon, R. Hessler, T. Juteau, M. Kastner, R. Larson, B. Luyendyk, J. D. McDougall, S. Miller, W. Normark, J. Orcutt, and C. Rangin. 1980. East Pacific Rise: hot springs and geophysical experiments. *Science* 207:1421-1433.
- Stauffer, D., and A. Aharony. 1994. *Introduction to Percolation Theory* Taylor & Francis, London.
- Strogatz, S. H. 2001. Exploring complex networks. *Nature* 410:268-76.
- Tunnicliffe, V. 1997. Hydrothermal vents: A global ecosystem. *JAMSTEC Journal of Deep-Sea Research*:105-110.
- Tunnicliffe, V., and C. M. R. Fowler. 1996. Influence of sea-floor spreading on the global hydrothermal vent fauna. Pages 531-533 *in* *Nature*.
- Tunnicliffe, V., C. M. R. Fowler, and A. G. McArthur. 1996. Plate tectonic history and hot vent biogeography. Pages 225-238 *in* *Tectonic, Magmatic, Hydrothermal and Biological Segmentation of Mid-Ocean Ridges* (C. J. MacLeod, P. A. Tyler, and C. L. Walker, eds.). Geological Society.
- Tunnicliffe, V., A. G. McArthur, and D. McHugh. 1998. A biogeographical perspective of the deep-sea hydrothermal vent fauna. *Advances in Marine Biology* 34:353-442.

- Urban, D., and T. Keitt. 2001. Landscape connectivity: A graph-theoretic perspective. *Ecology* 82:1205-1218.
- Van Dover, C. L. 1995. Ecology of Mid-Atlantic Ridge hydrothermal vents. Pages 257-294 *in* Hydrothermal vents and processes (L. M. Parson, C. L. Walker, and D. R. Dixon, eds.). Geological Society Special Publication, London.
- Van Dover, C. L. 2000. *The Ecology of Deep-Sea Hydrothermal Vents*. Princeton University Press, Princeton New Jersey.
- Van Dover, C. L., C. R. German, K. G. Speer, L. M. Parson, and R. C. Vrijenhoek. 2002. Evolution and biogeography of deep-sea vent and seep invertebrates. *Science* 295:1253-7.
- Van Dover, C. L., and R. R. Hessler. 1990. Spatial variation in faunal composition of hydrothermal vent communities on the East Pacific rise and Galapagos spreading center. Pages 253-264 *in* Gorda Ridge : A seafloor spreading center in the United States' exclusive economic zone (G. R. McMurray, ed.) Springer Verlag.
- Vrijenhoek, R. C. 1997. Gene flow and genetic diversity in naturally fragmented metapopulations of deep-sea hydrothermal vent animals. *Heredity* 88:285-293.
- Watts, D. J., and S. H. Strogatz. 1998. Collective dynamics of 'small-world' networks. *Nature* 393:440-2.

## Figures

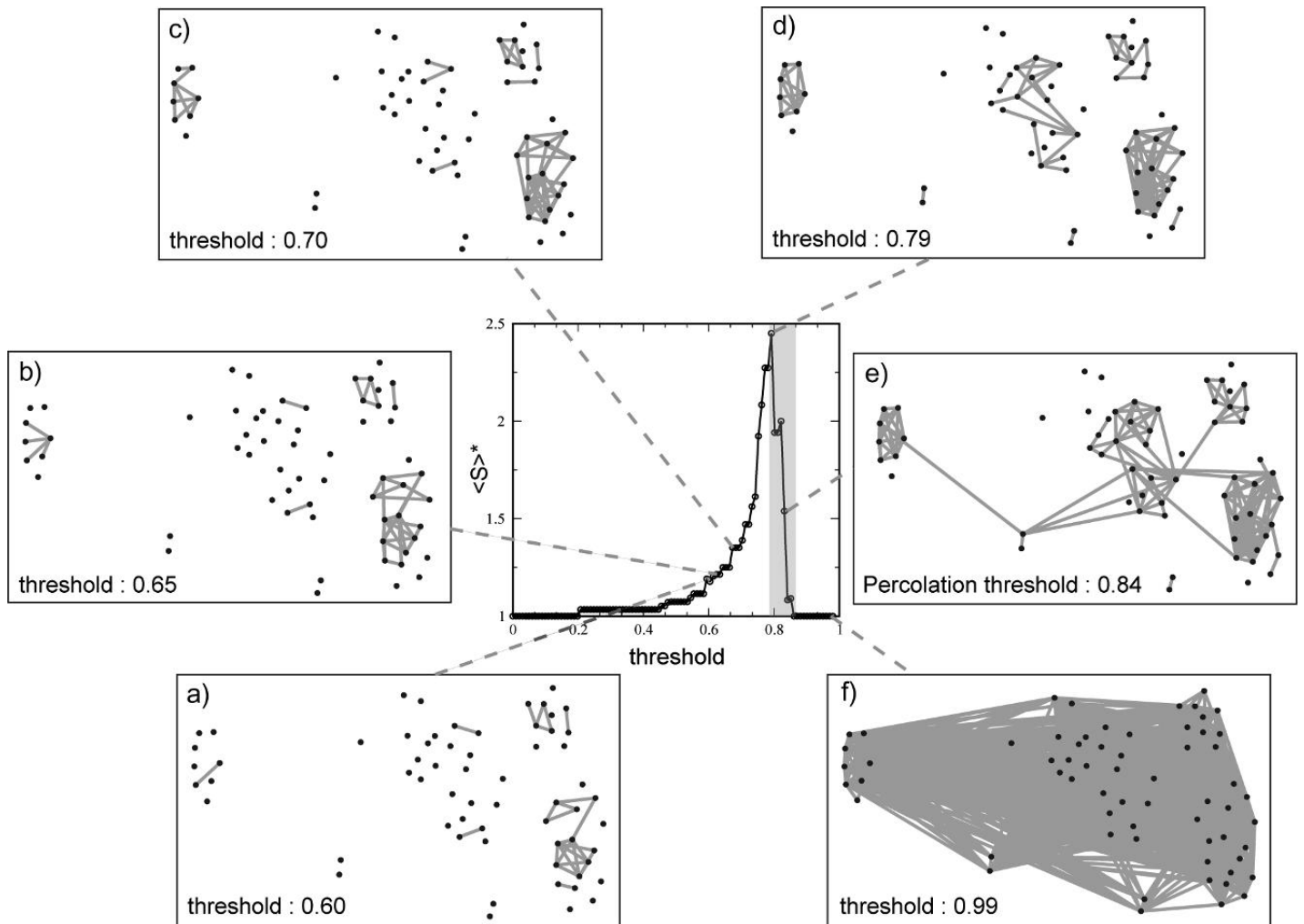


FIGURE 1. Evolution of network topology according to the average cluster size imposed by the Jaccard's distance at the genus level. Six threshold values were selected to visualize networks as a function of the average cluster size, excluding the largest one. The critical point is the Percolation Threshold. It is located in the transitional region (gray area). Percolation Threshold is reached just after all the clusters become connected. In our study, this critical value is 0.84. Each hydrothermal field is represented by a node, and the networks are distorted to accommodate the geographical distribution of hydrothermal sites. Link lengths are meaningless and only their presence/absence is finally taken into account in function of the threshold distance applied.

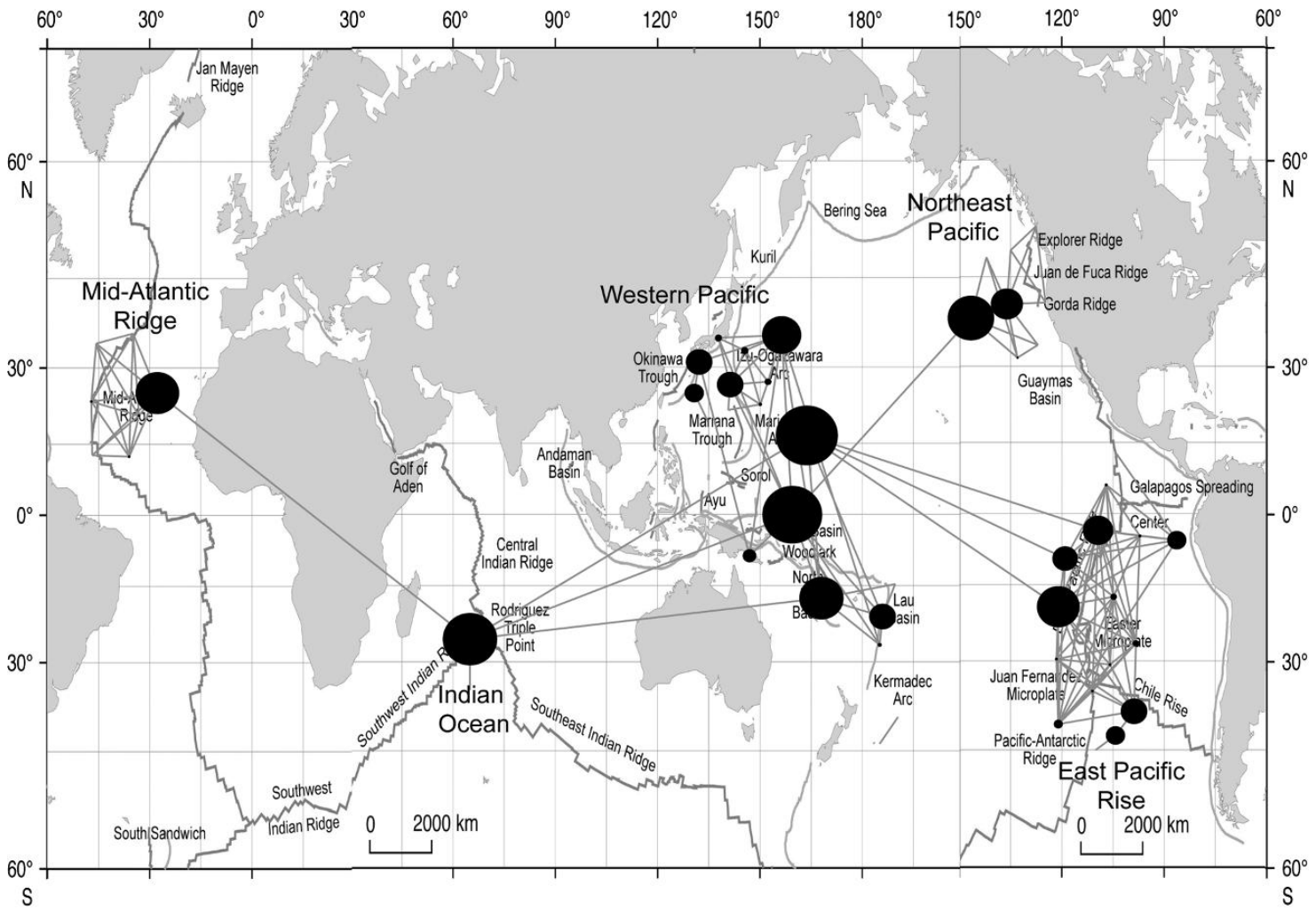


FIGURE 2. Global network of hydrothermal vent fauna diversity built on the basis of Jaccard's distance among fields and represented here at the percolation threshold ( $D_p = 0.84$ ). See Materials and Methods section). Circle size represents the betweenness centrality values of the corresponding field. Five provinces are highlighted by this network analysis: MAR, IO, WP, NP, and EPR.

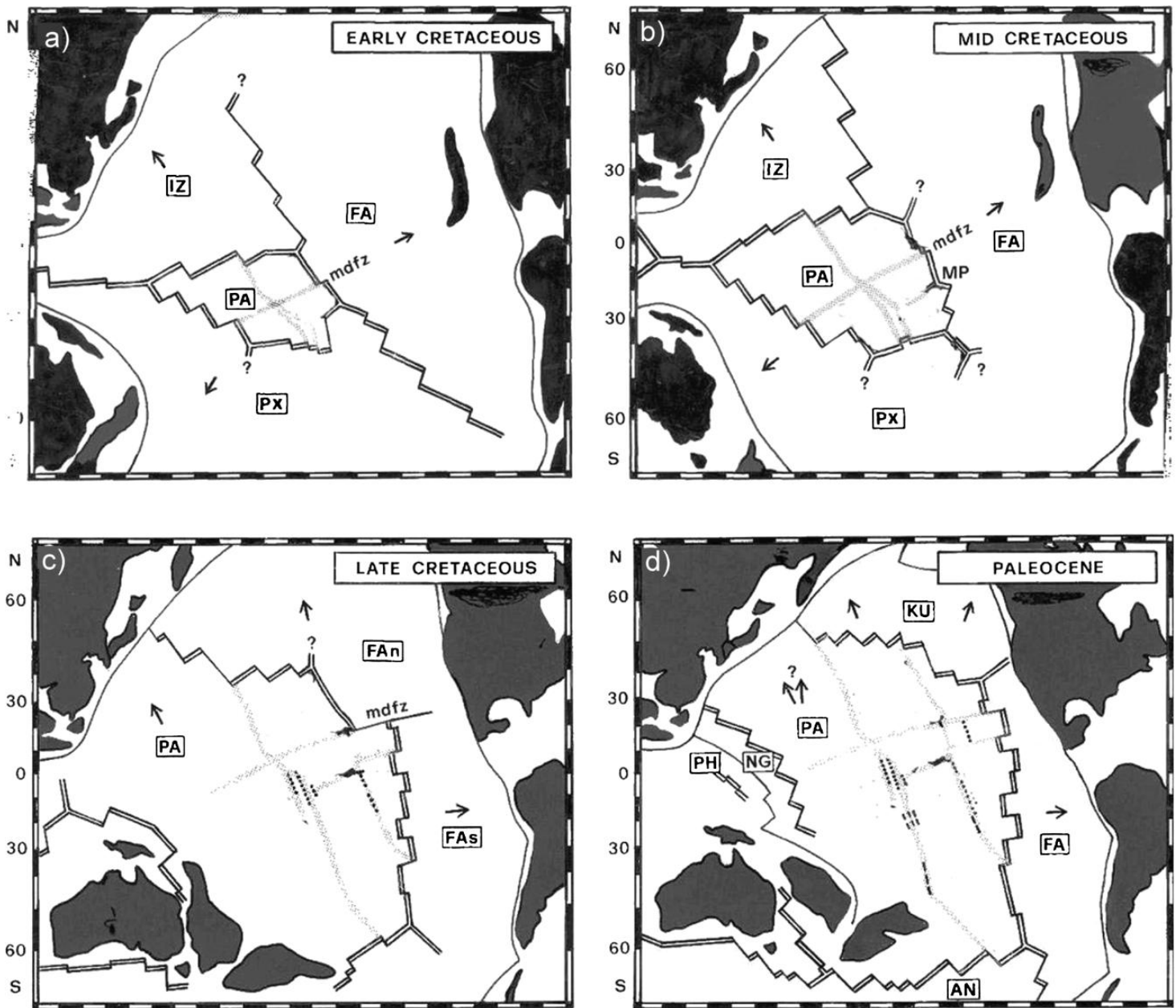


FIGURE 3. Evolution of the Pacific Basin from Early Cretaceous through Paleocene (modified from Smith (2003)) Abbreviations: AN = Antarctic; FA = Farallon (FAn = north, FAs = south); IZ = Izanagi; KU = Kula; NG = North New Guinea; PA = Pacific; PH = Philippine; PX = Phoenix. mdfz = Mendocino fracture zone. a) Early Cretaceous (140–130 Ma), b) Mid-Cretaceous (130–100 Ma), c) Late Cretaceous (approximately 83 Ma immediately prior to the formation of the Kula plate), d) Paleocene (approximately 60 Ma). The Kula plate has formed from the North Farallon plate.

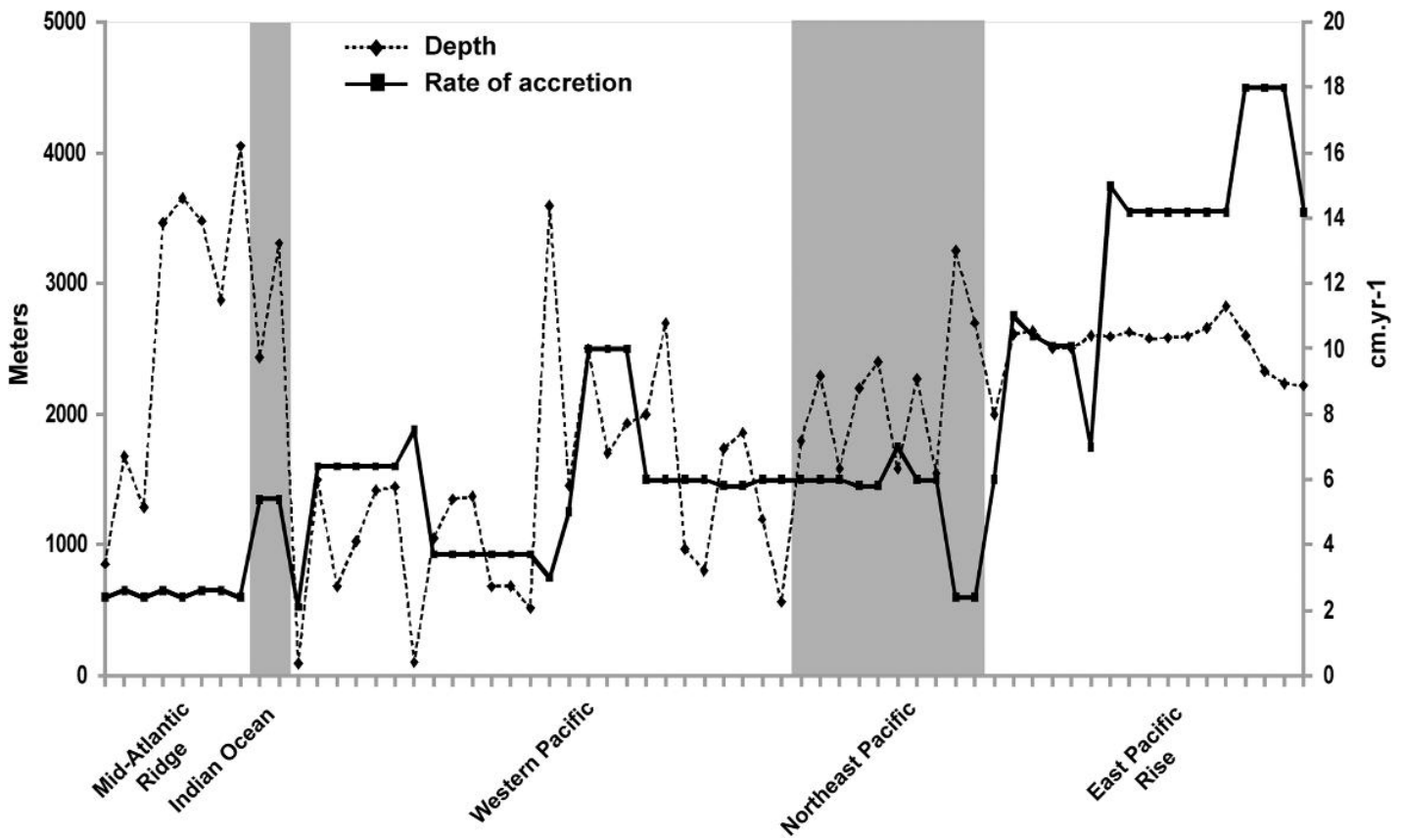


FIGURE 4. Codistribution of depth (dotted line) and rate of accretion (solid line) among the 63 fields. Depth scale is represented on the left y-axis and rate of accretion on the right y-axis. The field order is similar to the one in Table S3 and corresponds to the successive biogeographic provinces, separated by contrasted background on the graph.

## Supplementary Materials

### Supplementary Figures Captions

**Supplementary Figure 1.** Illustrations of network properties. a) Example of Clustering coefficient evolution on an undirected graph of 4 nodes. The local clustering coefficient of the black node is given for each graphs according to the links relying its neighbors (grey nodes connected by grey links). The clustering coefficient  $C$  is the proportion of existing connections between grey nodes compared with the total number of all possible connections. When  $C=0$ , there is no connection between the grey nodes among the 3 potential ones (grey dash lines). For  $C=1/3$ , there is only one connection on the 3 possible. When all the grey nodes are interconnected to each other,  $C=1$ . b) Example of Betweenness centrality (BC) values on an undirected graph of 13 nodes. The local betweenness centrality value of a node is calculated as the proportions of shortest paths between other node that go through it. Here, the BC values are 0 ( $BC=0/66$ ), 0.17( $BC=11/66$ ) and 0.91( $BC=60/66$ ) according to white, grey and black nodes respectively.

**Supplementary Figure 2.** Province endemism per genera a) and species b).  $n$  is the total number of entities observed inside each of the provinces symbolized by a chart. For each of the chart, light grey represents the percentage of endemic entities only observed in one field, grey is the percentage of entities shared inside the province and dark grey corresponds to the percentage of entities observed outside the provinces.

**Supplementary Figure 3.** Example of classical Multivariate exploratory techniques: Cluster analysis. A dichotomic diagram tree was built from the same distance matrix

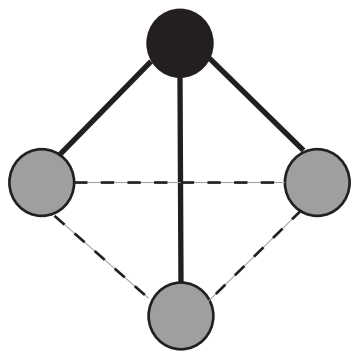
used for network analysis. Each of the 63 fields is plot on the left of the diagram. The linkage distance corresponds to Jaccard's distance. Colored branches match to the biogeographical provinces found with network analysis. Red for the Indian Ocean, yellow for the West-Pacific, brown for the Mid-Atlantic Ridge, green for the Northeast-Pacific and Blue for the East Pacific Rise. Black branches are the one that are connected aside the major cluster of the tree. It can be noted that some of the identified provinces are here “polyphyletic”, therefore the difficulties in defining them on the basis of that kind analysis.

**Supplementary Figure 4.** World-wide network of the hydrothermal vents fauna diversity (Species Level). Network built on the basis of Jaccard distance among fields and represented here at the percolation threshold ( $D_p=0.95$ ). Circle size illustrates the betweenness centrality values of the corresponding field. The same five provinces found at the genera level are highlighted by this network analysis: the Mid-Atlantic Ridge, the Indian Ocean, the Western-Pacific, the Northeast-Pacific and the East Pacific Rise.

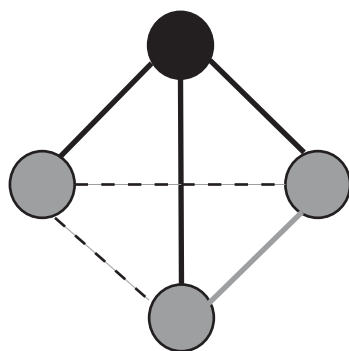
**Supplementary Figure 5.** Evolution of network topology according to the average cluster size imposed by the Jaccard's distance at the species level. Six thresholds values were selected to visualize networks in function of the average cluster size excluding the largest one. The critical point is the Percolation Threshold. It is located in the transitional region (grey area). It is reached just before all the clusters get disconnected. In this case, the critical value is 0.95.

**Supplementary Figure 6.** World-wide networks of the three major phylum hydrothermal vents fauna diversity at the Genera Level. a) Annelida, b) Arthropoda and c) Mollusca. Networks built on the basis of Jaccard distance among fields and represented here at their Percolation threshold. Circle size illustrates the betweenness centrality values of the corresponding field.

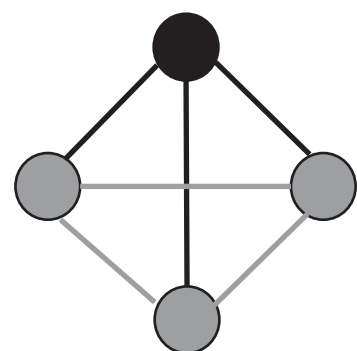
a)



**C=0**

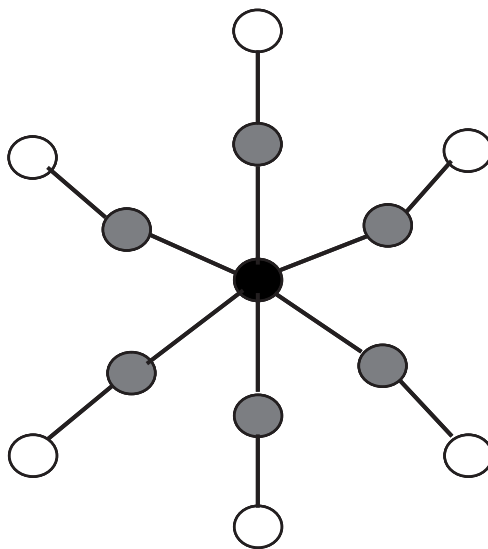


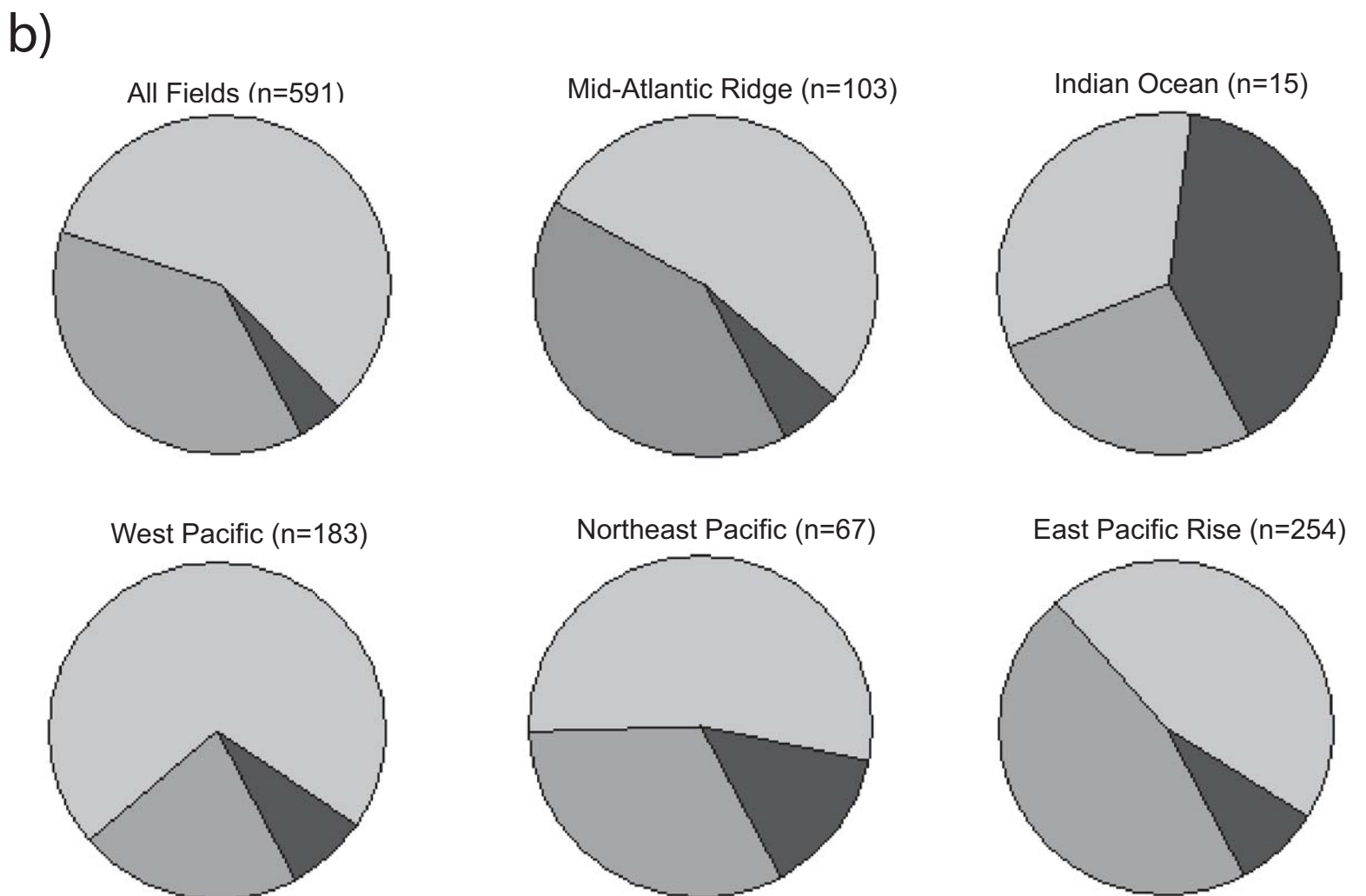
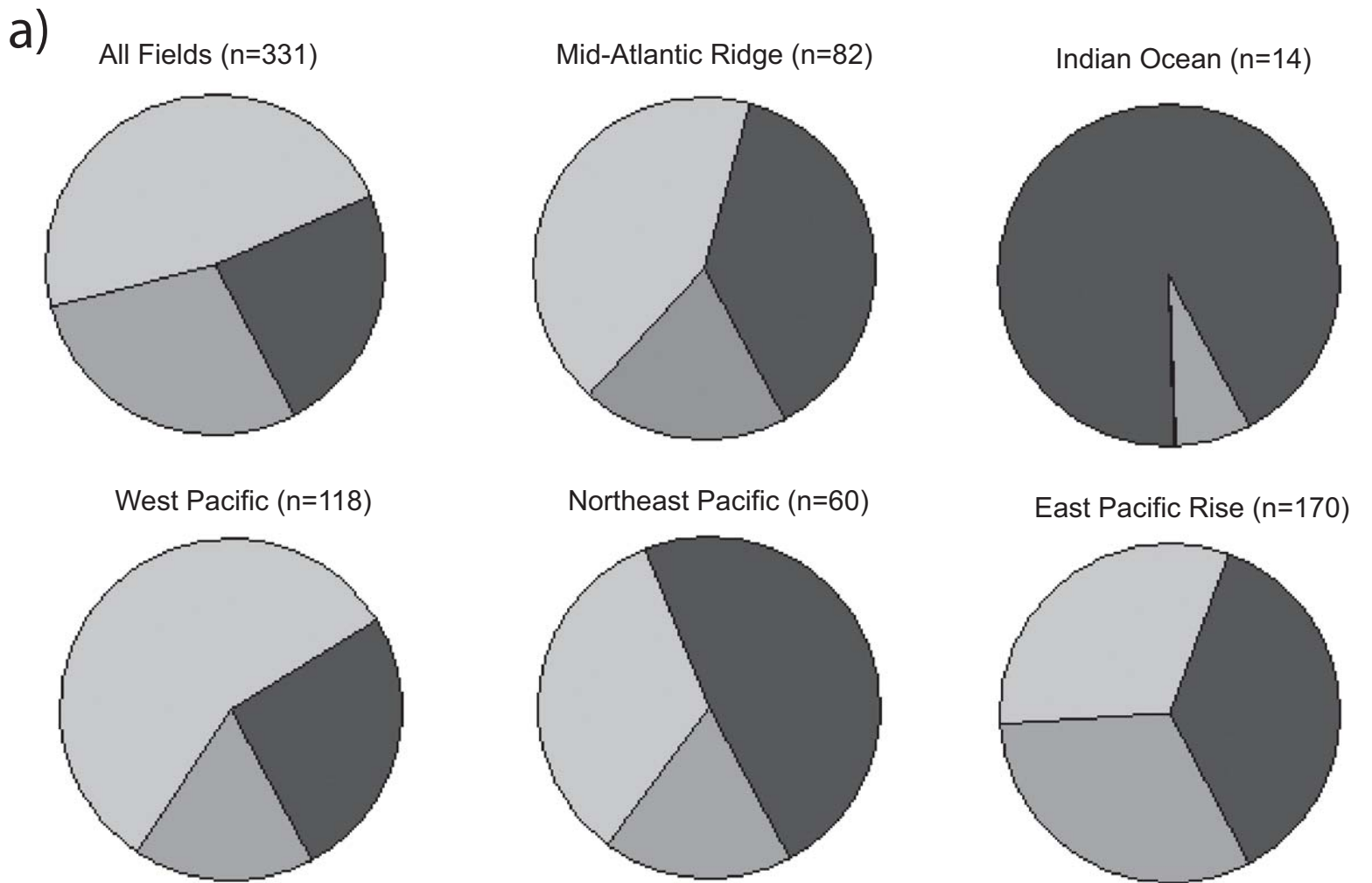
**C=1/3**



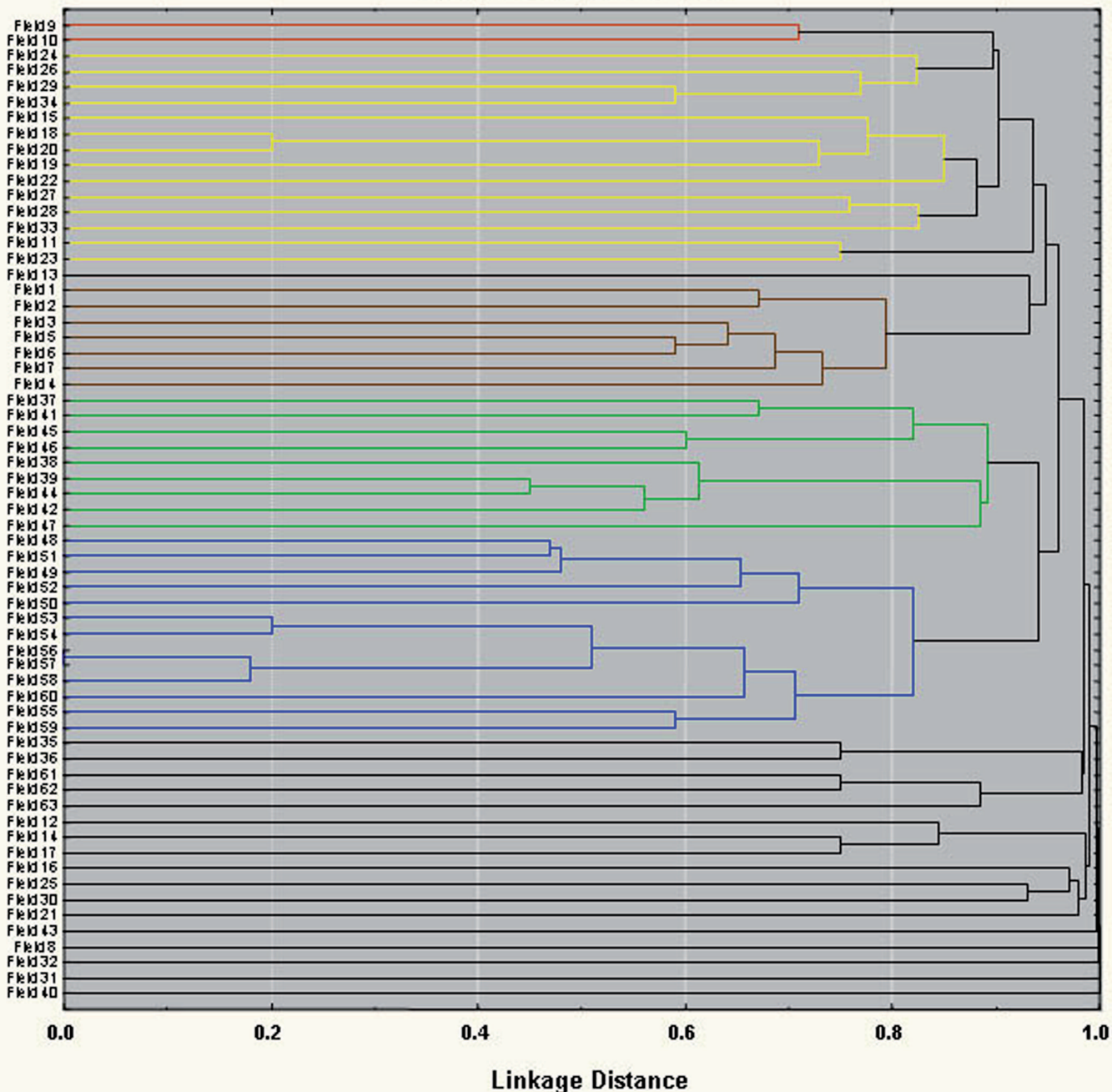
**C=1**

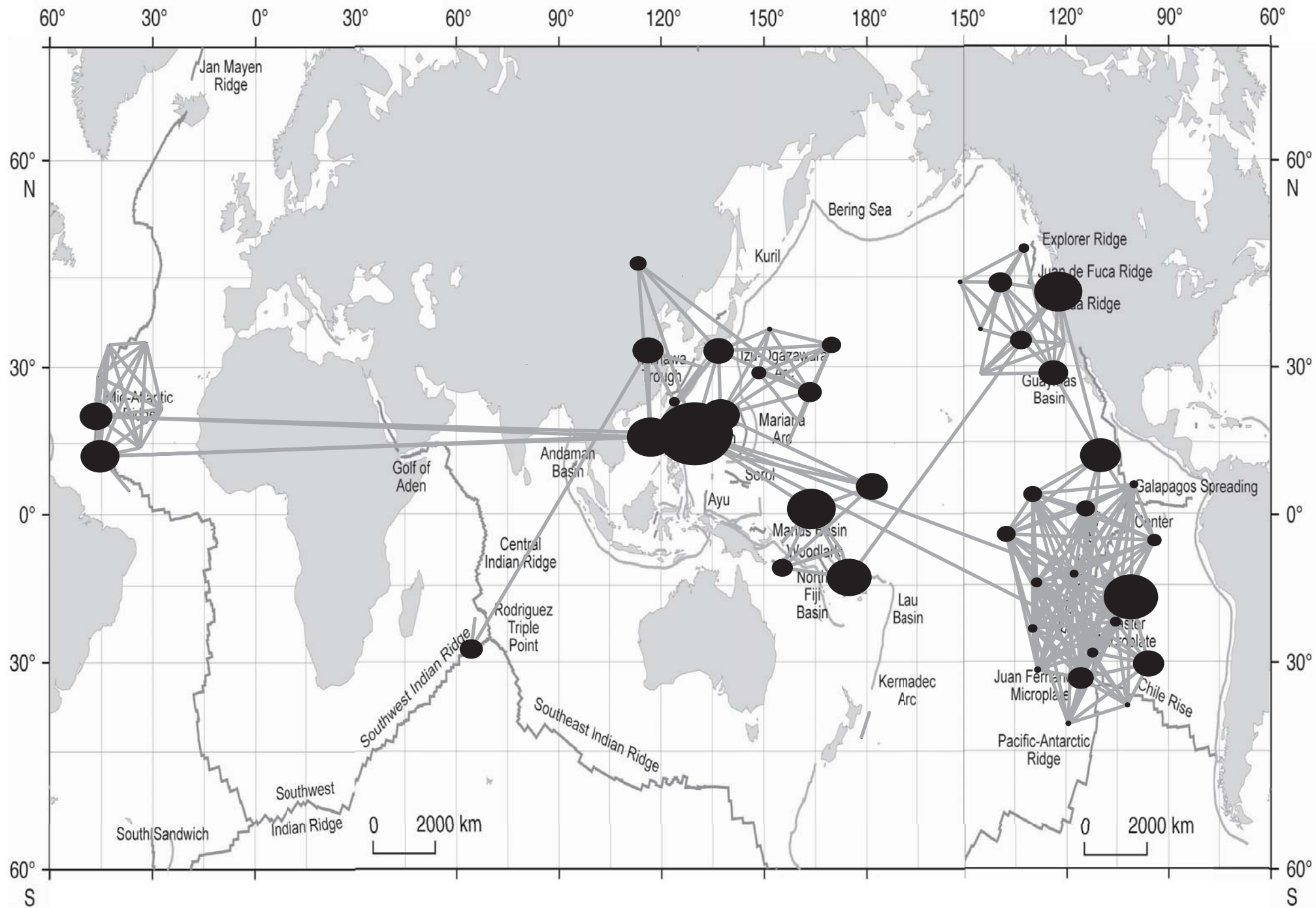
b)

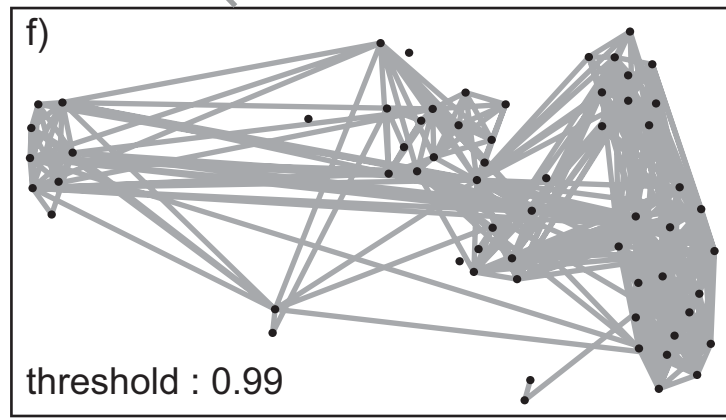
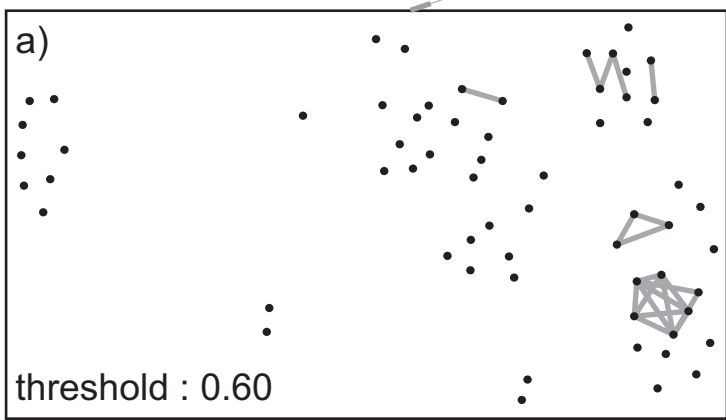
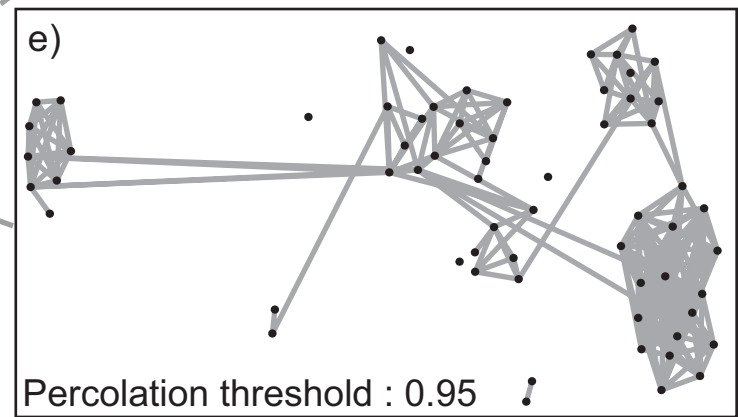
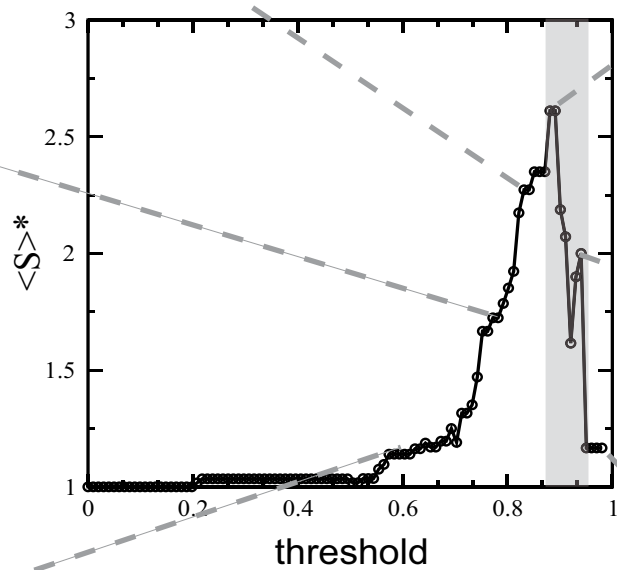
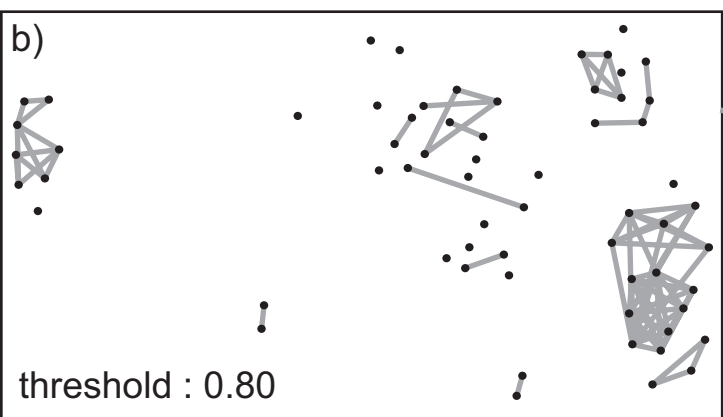
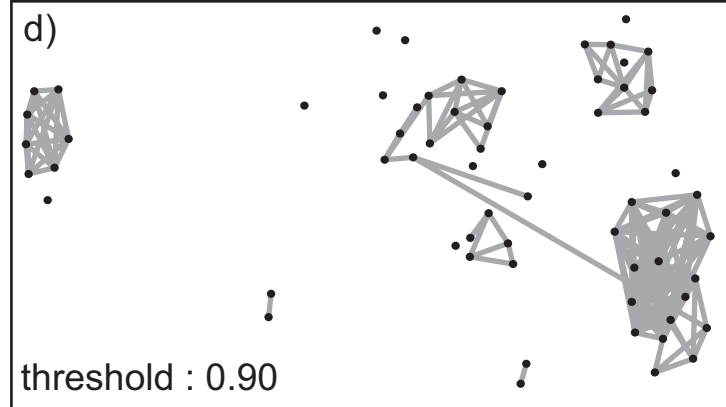
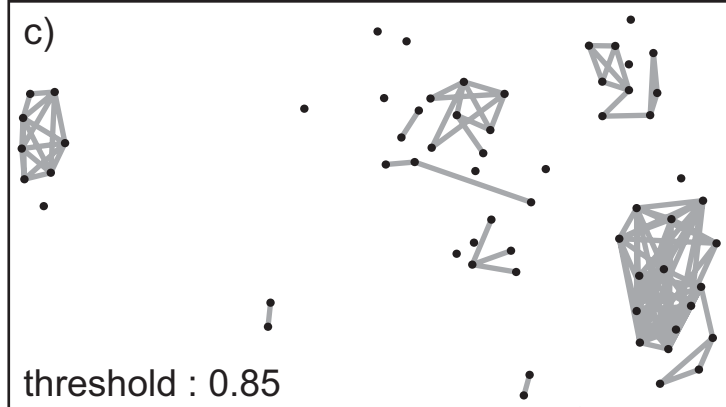


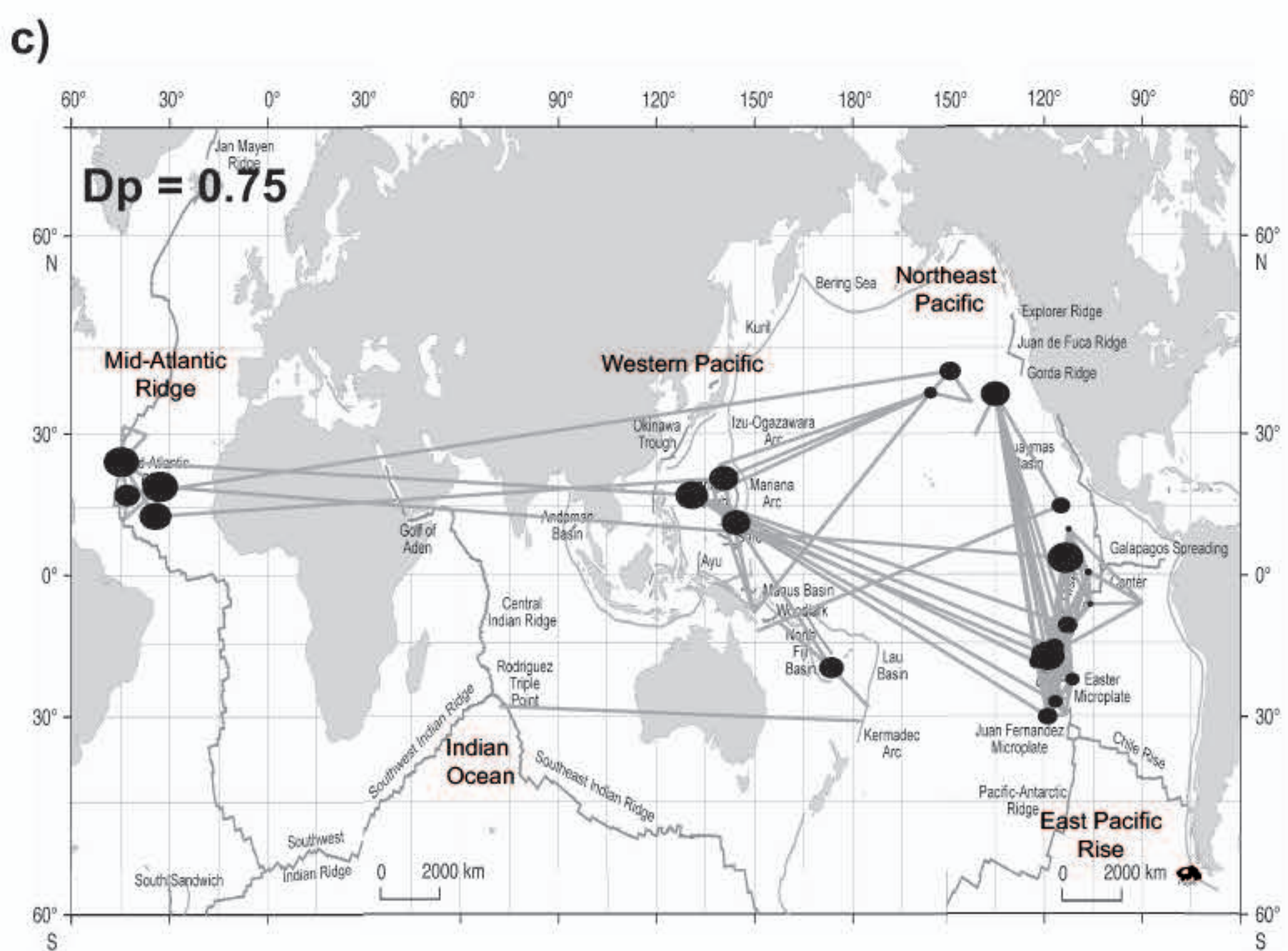
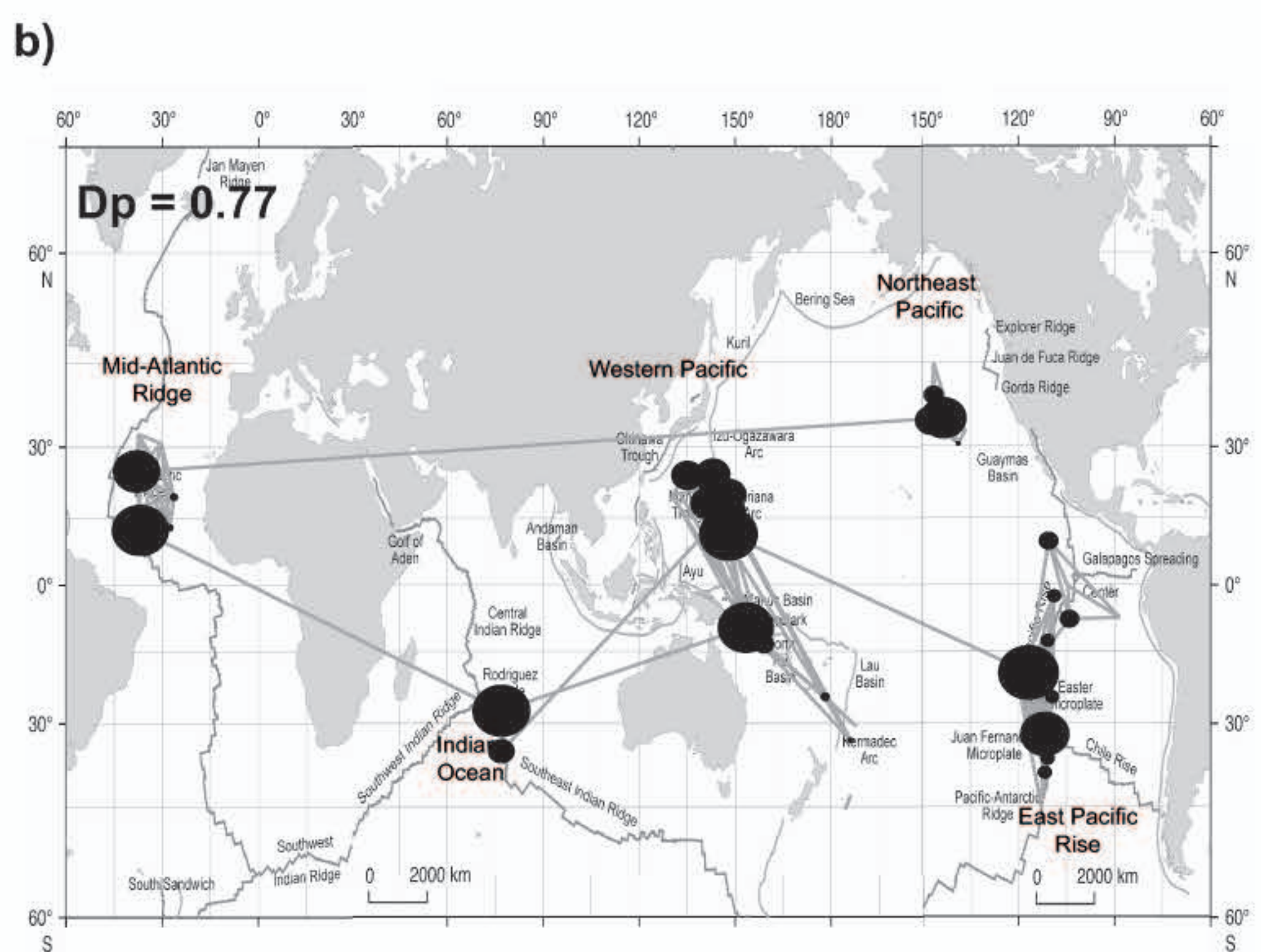
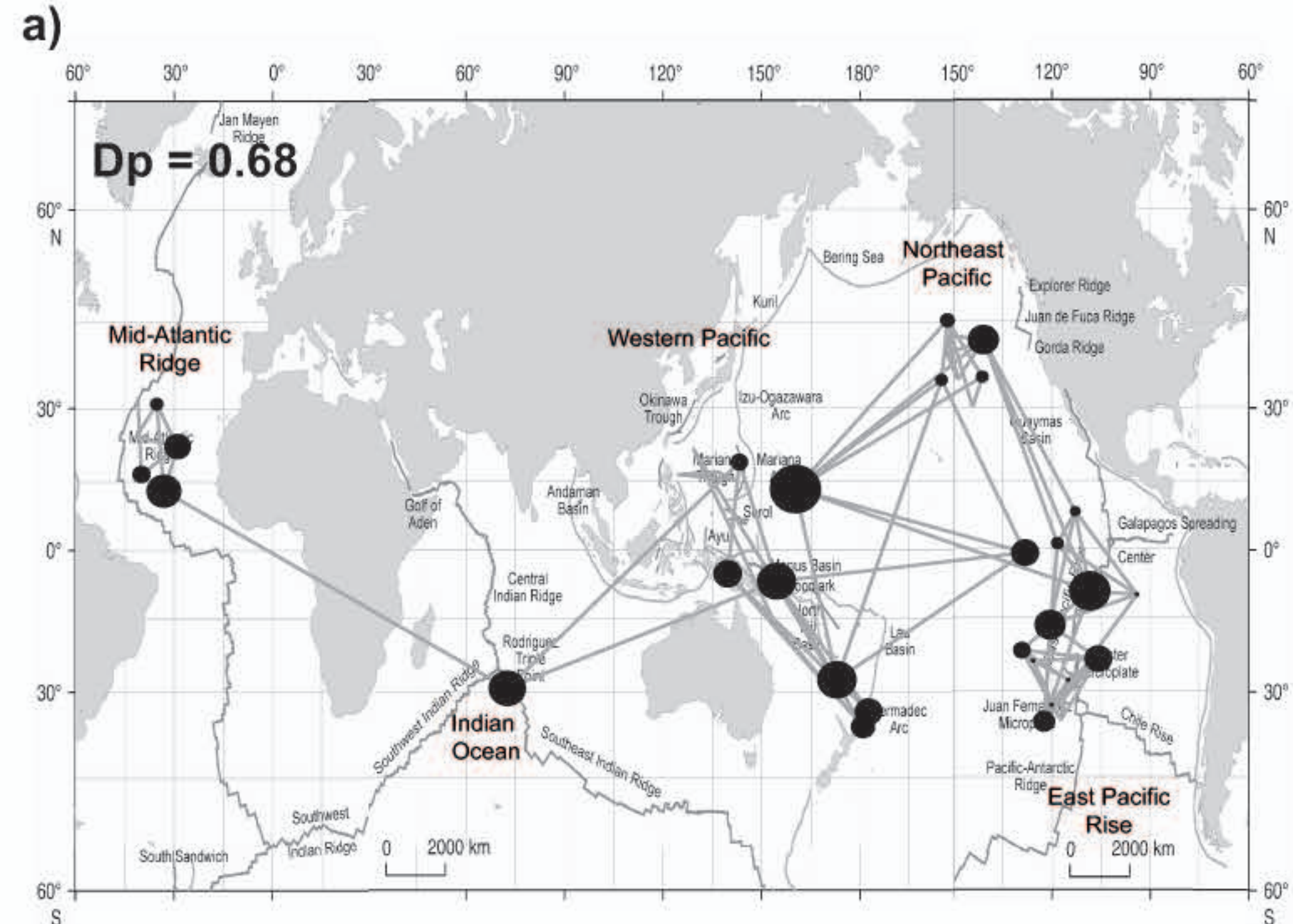


Tree Diagram for 63 HV Fields  
Unweighted pair-group average  
Dissimilarities from matrix









---

**Table 1 Network properties of identified provinces at the percolation threshold**

---

	Provinces				
	Mid-Atlantic Ridge	Indian Ocean	West Pacific	Northeast Pacific	East Pacific Rise
n	8	2	26	10	17
Cluster size	7	2	17	8	16
BC max/<BC>	0.14/0.017*	0.21/0.107* <sup>†</sup>	0.28/0.038***	0.16/0.023**	0.13/0.021***
<k>	5.57	3.00	4.53	3.88	7.81
<CC>	0.92	-	0.68	0.88	0.81

---

n is the number of fields localized inside the province, cluster size is the effective number of fields within the "province" cluster at the percolation threshold. For each province, <k> is the average connectivity degree, BC max is the maximum value of betweenness centrality and <CC> is the average value of clustering coefficient. *p-values* \* $<0.1$ , \*\* $<0.05$ , \*\*\* $<0.001$ . <sup>†</sup> the mean value for IO is based on only two sampled fields, and is therefore subject to high variance.

used for network analysis. Each of the 63 fields is plot on the left of the diagram. The linkage distance corresponds to Jaccard's distance. Colored branches match to the biogeographical provinces found with network analysis. Red for the Indian Ocean, yellow for the West-Pacific, brown for the Mid-Atlantic Ridge, green for the Northeast-Pacific and Blue for the East Pacific Rise. Black branches are the one that are connected aside the major cluster of the tree. It can be noted that some of the identified provinces are here “polyphyletic”, therefore the difficulties in defining them on the basis of that kind analysis.

**Supplementary Figure 4.** World-wide network of the hydrothermal vents fauna diversity (Species Level). Network built on the basis of Jaccard distance among fields and represented here at the percolation threshold ( $D_p=0.95$ ). Circle size illustrates the betweenness centrality values of the corresponding field. The same five provinces found at the genera level are highlighted by this network analysis: the Mid-Atlantic Ridge, the Indian Ocean, the Western-Pacific, the Northeast-Pacific and the East Pacific Rise.

**Supplementary Figure 5.** Evolution of network topology according to the average cluster size imposed by the Jaccard's distance at the species level. Six thresholds values were selected to visualize networks in function of the average cluster size excluding the largest one. The critical point is the Percolation Threshold. It is located in the transitional region (grey area). It is reached just before all the clusters get disconnected. In this case, the critical value is 0.95.

**Supplementary Figure 6.** World-wide networks of the three major phylum hydrothermal vents fauna diversity at the Genera Level. a) Annelida, b) Arthropoda and c) Mollusca. Networks built on the basis of Jaccard distance among fields and represented here at their Percolation threshold. Circle size illustrates the betweenness centrality values of the corresponding field.

---

**Supplementary Table 1. Number of genera per phylum in each identified provinces**

---

	Provinces					All Fields
	Mid-Atlantic Ridge	Indian Ocean	West- Pacific	Northeast Pacific	East-Pacific Rise	
Arthropoda	40	7	38	17	54	122
Mollusca	17	5	41	20	39	83
Annelida	8	1	23	21	45	67
Chordata	4	0	7	0	8	16
Cnidaria	6	1	2	0	8	15
Porifera	2	0	4	0	5	9
Echinodermata	2	0	1	0	4	6
Nematoda	1	0	2	0	3	5
Foraminiferida	1	0	0	0	1	2
Ciliophora	0	0	0	1	0	1
Nemertea	0	0	0	1	0	1
Acanthocephala	0	0	0	0	1	1
Hemicordata	0	0	0	0	1	1
macnabi	0	0	0	0	1	1
Chaethognata	1	0	0	0	0	1
genera number	82	14	118	60	170	331

---

**Supplementary Table 2. Comparative analyses of different communities detection method.**

<b>Title of the method</b>	<b>Description</b>	<b>Results</b>	<b>Reference</b>
Maps of information flow reveal community structure in complex networks	Use of probability flow of random walks on a network as a proxy for information flows in the real system and decompose the network into modules by compressing a description of the probability	3 clusters but congruent with the percolation network topology: Cluster1: MAR-IO-WP Cluster2: NP Cluster3: EPR Preferential connections order: Cluster1-Cluster2> Cluster1-Cluster3> Cluster2-Cluster3	<b>Rosvall and Bergstrom, 2008<sup>a</sup></b>
Fast unfolding of communities in large network	Based on two iterative phases repeat until no increase of modularity: First, modularity optimization. Second, communities aggregation.	1 single giant cluster, unresolved	<b>Blondel et al., 2008<sup>b</sup></b>
Graph Clustering Via a Discrete Uncoupling Process	A Markov Cluster Algorithm that simulates (stochastic) flow in graphs based on expansion and inflation. Eventually, iterating expansion and inflation results in the separation of the graph into different segments (clusters)	Unresolved biogeographic provinces: Cluster1: WP-NP-EPR-MAR Cluster2: IO-WP Cluster3: WP Cluster4: WP	<b>Dongen, 2008<sup>c</sup></b>
Community structure in social and biological networks	Based on edge "betweenness" centrality to find community boundaries	1 single "giant" cluster only resolved when analyzing at the percolation point where the same clusters/provinces were identified as the ones in the simple percolation analysis	<b>Girvan and Newman, 2002<sup>d</sup></b>

<sup>a</sup> Rosvall, M., and C. T. Bergstrom. 2008. Maps of random walks on complex networks reveal community structure. *Proc Natl Acad Sci U S A* 105:1118-23.

<sup>b</sup> Blondel, V. D., J. L. Guillaume, R. Lambiotte, and E. Lefebvre. 2008. Fast unfolding of communities in large networks. *Journal of Statistical Mechanics-Theory and Experiment*

<sup>c</sup> Dongen, S. V. 2008. Graph Clustering Via a Discrete Uncoupling Process. *SIAM Journal on Matrix Analysis and Applications* 30:121-141

<sup>d</sup> Girvan, M., and M. E. Newman. 2002. Community structure in social and biological networks. *Proc Natl Acad Sci U S A* 99:7821-6

**Supplementary Table 3. Hydrothermal vents fields used in this study**

Field (abbreviation)	Ridge	Latitude deg-min	Longitude deg-min	Field number on map	Depth meter	Rate of accretion cm.yr <sup>-1</sup>
Menez Gwen (MG)	Mid-Atlantic Ridge	37°51N	31°31W	1	853	2.4
Lucky Strike (LS)	Mid-Atlantic Ridge	37°17N	32°16W	2	1675	2.6
Rainbow (Rb)	Mid-Atlantic Ridge	37°30N	33°54W	3	1285	2.4
Broken Spur (BS)	Mid-Atlantic Ridge	29°10N	43°10W	4	3463	2.6
TAG (TAG)	Mid-Atlantic Ridge	26°08N	44°49W	5	3653	2.4
Snake Pit (SP)	Mid-Atlantic Ridge	23°23N	44°58W	6	3480	2.6
Logatchev (Log)	Mid-Atlantic Ridge	14°45N	44°58W	7	2875	2.6
Ashadze 1 (A1)	Mid-Atlantic Ridge	12°58N	44°52W	8	4050	2.4
Kairei Vent Field (KVF)	Central Indian Ridge	25°19S	70°02E	9	2438	5.4
Edmond Vent Field (EVF)	Central Indian Ridge	23°52S	69°35E	10	3305	5.4
Kagoshima Bay (KB)	Japan Ridge	31°39N	130°48E	11	96	2.1
Hatoma Knoll (HK)	Okinawa Trough	28°24N	123°50E	12	1495	6.4

Minami-Ensei Knoll (MEK)	Okinawa Trough	28°24N	127°38E	13	680	6.4
North Iheya Knoll (NIK)	Okinawa Trough	27°47N	126°54E	14	1030	6.4
Iheya Ridge (IR)	Okinawa Trough	27°33N	126°59E	15	1415	6.4
Izena Cauldron (IC)	Okinawa Trough	27°16N	127°05E	16	1445	6.4
Northeastern						
Taiwan (NET)	Okinawa Arc	24°50N	121°60E	17	100	7.5
Mokuyo Seamount (MS)	Izu-Ogasawara Arc	28°34N	140°39E	18	1050	3.7
Myojin Knoll (MK)	Izu-Ogasawara Arc	32°07N	139°51E	19	1350	3.7
Suiyo Seamount (SS)	Izu-Ogasawara Arc	28°34N	140°39E	20	1367	3.7
Sumisu Caldera (SC)	Izu-Ogasawara Arc	31°28N	140°04E	21	680	3.7
Kaikata Seamount (KS)	Izu-Ogasawara Arc	26°42N	141°04E	22	685	3.7
Nikko Seamount (NS)	Izu-Ogasawara Arc	23°06N	142°40E	23	515	3.7
Mariana	Mariana Back-Arc	18°12N	144°42E	24	3595	3

Trough (MT)	Basin					
Edison Seamount (EDS)	Tabar-Feni Volcanic Fore Arc	03°01S	152°03E	25	1450	5
Vienna Woods (VW)	Manus Back-Arc Basin	03°09S	150°16E	26	2500	10
Pacmanus Complex (PC)	Manus Back-Arc Basin	03°43S	151°40E	27	1700	10
Desmos Cauldron (DC)	Manus Back-Arc Basin	03°41S	151°52E	28	1930	10
White Lady (WL)	North-Fiji Back-Arc Basin	16°59S	173°55E	29	2000	6
Mussel Valley (MV)	North-Fiji Back-Arc Basin	18°49S	173°29E	30	2700	6
Loihi Seamount (LOS)	Intra-Plate Seamount	18°57N	155°16W	31	969	6
Vailulu'u Seamount (VS)	Intra-Plate Seamount	14°13S	169°04W	32	800	6
Vai Lili (VL)	Lau Back-Arc Basin	22°13S	176°37W	33	1736	5.8
Hine Hina (HH)	Lau Back-Arc Basin	22°32S	176°43W	34	1860	5.8
Brothers Seamount	Kermadec Arc	34°52S	179°04E	35	1197	6

(BRS)						
Rumble V Seamount (RVS)	Kermadec Arc	36°08S	178°11E	36	561	6
Magic Mountain (MM)	Explorer	49°46N	130°15W	37	1797	6
Middle Valley (MIV)	Juan de Fuca	48°27N	128°42W	38	2291	6
Endeavour Segment (ES)	Juan de Fuca	48°00N	129°04W	39	1580	6
Coaxial Segment (CAS)	Juan de Fuca	46°19N	129°42W	40	2200	5.8
Axial-Volcano (AV)	Juan de Fuca	45°55N	129°59W	41	2400	5.8
Axial Volcano Coaxial Seamount (AVCASM)	Juan de Fuca	45°59N	130°02W	42	1580	7
Axial Volcano Ashes Vent Field (AVAVF)	Juan de Fuca	45°56N	130°00W	43	2270	6
Cleft Segment (CS)	Juan de Fuca	44°39N	130°15W	44	1547	6
Sea Cliff Vent Field (SCVF)	Gorda	42°15N	126°42W	45	3250	2.4

Escabana Trough (ET)	Gorda	41°00N	127°29W	46	2700	2.4
Guaymas Basin (GB)	Gulf of California	27°00N	111°24W	47	2000	6
21°N (21N)	Northern East- Pacific Rise	20°50N	109°06W	48	2615	11
13°N (13N)	Northern East- Pacific Rise	12°50N	103°57W	49	2635	10.4
11°N (11N)	Northern East- Pacific Rise	11°23N	103°46W	50	2504	10.1
9°N (9N)	Northern East- Pacific Rise	09°49N	104°17W	51	2500	10.1
Galapagos Spreading Center (GSC)	Galapagos	00°48N	86°10W	52	2601	7
7°S (7S)	Southern East- Pacific Rise	07°21S	107°47W	53	2594	15
14°S (14S)	Southern East- Pacific Rise	13°58S	112°28W	54	2629	14.2
17°S (17S)	Southern East- Pacific Rise	17°24S	113°12W	55	2580	14.2
17°24S (1724S)	Southern East- Pacific Rise	17°25S	113°12W	56	2583	14.2

17°34S (1734S)	Southern East- Pacific Rise	17°34S	113°14W	57	2595	14.2
18°S (18S)	Southern East- Pacific Rise	18°24S	113°24W	58	2658	14.2
21°S (21S)	Southern East- Pacific Rise	21°25S	114°17W	59	2825	14.2
23°S (23S)	Southern East- Pacific Rise	23°32S	115°34W	60	2598	18
31°S (31S)	Southern East- Pacific Rise	31°09S	111°55W	61	2330	18
Saguaro Field (SF)	Southern East- Pacific Rise	31°51S	112°02W	62	2235	18
German Flats (GF)	Southern East- Pacific Rise	37°47S	110°55W	63	2216	14.2

---

---

**Supplementary Table 4. Key fields in relaying information**

---

	Provinces								
	Mid-Atlantic Ridge	Indian Ocean	West Pacific			Northeast Pacific	East-Pacific Rise		
Key Fields	3	9	24	27	29	41	50	51	55
BC_value/	0.14/	0.21/	0.28/	0.26/	0.14/	0.16/	0.07/	0.05/	0.13/
Provinces_connection	IO	MA&WP	IO&EPR	IO&NP	IO	WP	WP	WP	WP

---

## Glossary

**Betweenness centrality:** the fraction of the shortest paths in the network to pass through a node.

**Clustering coefficient:** a measure of the proportion neighboring nodes that can be reached through the nodes of other neighbors; calculated as the proportion of the focal node neighbors that are themselves neighbors.

**Degree of connectivity:** number of edges that connect the focal node to other nodes.

**Edge:** a connection between interacting nodes

**Node:** an individual element within a network

**Shortest path:** the path that traverses the minimum number of edges between two nodes